

MÁSTERES de la UAM

Facultad de
Ciencias / 16-17

Física Teórica

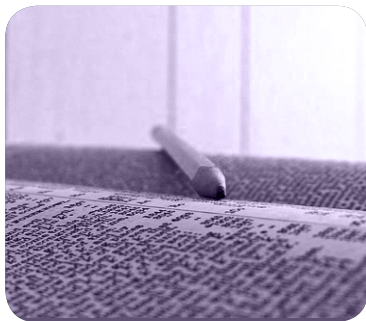


Campus Internacional
excelencia UAM
CSIC+



Multi-Field Inflation From Moduli Stabilization

*Eduardo Gonzalo
Badía*



Multi-Field Inflation From Moduli Stabilization

MSc Thesis

Author: **Eduardo Gonzalo Badía**

Supervisors: **Clemens Wieck, Francisco Pedro**

Master in Theoretical Physics at Instituto de Física Teórica (IFT)
and Universidad Autónoma de Madrid (UAM)



August 29, 2017

Abstract

In the context of inflationary model building it is well known that curvature and isocurvature perturbations can couple when more than one scalar field is present. It is also known that multiple scalar fields arise naturally in String Theory models of Inflation. First we review the necessary tools to extract predictions for the cosmological observables for multi-field inflationary models. After testing the code with examples from the literature we study a particular large-field toy model which is a low-energy effective theory that can arise in various string compactifications. Generalizing the analysis in [1–7], in [8] the one-loop corrections to the instanton action were included in the non-perturbative term of the superpotential. In the example we study here, this induces periodic modulations in the inflationary scalar potential. In particular, we consider Type IIB flux compactifications where one field parameterizes the volume of a four-cycle in the compact manifold Y_6 and the other is the position modulus of a D7-brane, also wrapping a four-cycle. Finally, we use data from the CMBR and LSS observations to study the viability of this model.

Contents

1	Introduction	1
2	Cosmology	5
2.1	The Standard Model of Cosmology	5
2.2	The inflationary paradigm	5
2.3	Cosmological perturbation theory	7
2.4	Single-field Inflation	9
2.4.1	Classical theory	9
2.4.2	Quantum theory	10
2.4.3	Cosmological observables	11
3	Multi-field Inflation	13
3.1	Classical theory	13
3.2	Quantum theory	15
3.3	Cosmological observables	16
3.4	Numerical example	17
4	String Theory	20
4.1	Basics of String Theory	20
4.2	Type IIB Supergravity limit. Compactification. Moduli stabilization.	20
5	String Inflation	24
5.1	Motivation	24
5.2	Energy scales and challenges in String Inflation	24
6	Our Model	27
6.1	Motivation. Introducing one-loop corrections in W_{np}	27
6.2	Numerical evaluation	30
6.2.1	Small Γ and large δ	30

6.2.2	Large Γ and small δ	35
6.2.3	Large Γ and large δ	39
6.2.4	Comparing the examples	43
7	Conclusions	45

1 Introduction

The Standard Model of Cosmology (SMC) [9–11] is a widely accepted model of the large scale properties of the Universe, which is taken to be a perturbed Robertson-Walker space-time filled with quantum fields. On large scales this model is accepted because it is able to explain consistently observations from very different experiments such as CMBR observations from WMAP [12] and Planck [13], Large Scale Structure surveys such as SDSS [14], Gravitational Lensing CASTLES Survey [15] or type Ia supernovae [16]. On small scales it is accepted since the fundamental physics behind it is General Relativity (GR) plus a certain Quantum Field Theory known as the Standard Model of Particle Physics (SM).

However, we know that GR and QFT are not compatible at a fundamental level, and the SMC, as we know it, is expected to break down at an energy close to the Planck mass. Being based on GR, the SMC inherits its UV inconsistencies such as non-renormalizability and also the (at best unsettling) issue of the singularity at $t = 0$. For these reasons, it is widely believed that once a Quantum Theory of Gravity is established, the SMC will emerge as an effective theory valid only until an energy scale much smaller than the Planck mass. The periods preceding the SMC are known as *Inflation* and *Reheating*. Inflation is often assumed to start its description a bit below or at the Planck mass. The fundamental physics behind these periods is, at present, an open problem. Furthermore, unlike the SMC, they are still not accessible by experiments. This means that all evidence and experimental bounds we have on the physics of Inflation is based on indirect evidence. A discovery of a stochastic background of Primordial Gravitational Waves [17, 18] or B-modes in the CMB [19] in the future could provide key additional data. Although unlikely in the next few years, this would put strong constraints on most of the inflationary models studied so far.

The SMC is able to successfully account for almost all cosmological observations, but we have seen that it cannot be extrapolated to the very early Universe. This problem shows up in the form of unphysical, highly fine-tuned initial conditions. Namely, the SMC assumes that the Universe was incredibly flat and homogeneous in the past. This assumption is a severe shortcoming in the predictive power of the theory. Furthermore, since the comoving horizon is always increasing during the SMC, it cannot explain why regions of the Universe which were not in causal contact are observed to be homogeneous in up to 5 orders of magnitude. This problem is known as the horizon problem.

The inflationary paradigm [20–22] provides an explanation for these initial conditions and for the horizon problem through a period of almost exponential expansion in which the comoving horizon is decreasing. According to the paradigm, the Universe is assumed to be filled with scalar fields rolling down a certain potential. Like in the SMC, it is assumed to be isotropic and homogeneous at first order. The only initial conditions needed in the classical sense are

for the background quantities (i.e. the scalar fields and the geometry of the Universe). The initial conditions for the inhomogeneities appear naturally as the ground state of Quantum Mechanics. It is remarkable that the seeds of the CMB anisotropies and of all LSS may be the quantum fluctuations of the perturbations of the metric and matter content of the Universe. Unfortunately, as we have stated, there is still much uncertainty regarding the inflationary and reheating epochs.

The homogeneous evolution during the SMC is explained by the Λ CDM model, the acronym referring to the Dark Energy (Λ) and the Cold Dark Matter (CDM) and components. At present it remains to be seen whether SM physics (or a bit beyond it) will be sufficient to account for these two components. Since there is much uncertainty regarding Inflation and Reheating, it is remarkable that we have been able to find a set of *fundamental* parameters which are sufficient to make predictions. For the homogeneous background we need to specify initial conditions: i) for the metric (e.g. the Hubble parameter) and ii) for the particle, DM and DE content of the Universe. In order to make statistical predictions about the CMB (anisotropies in the power spectra) and Large Scale Structure (power spectra, BAO peak in the correlation function) we need one more function: the primordial power spectra of perturbations (PPSP). This function sets the initial conditions for the perturbations (including metric and density perturbations). This function is predicted by Inflation and it is the one that will concern us in this work.

Observations of the CMB and LSS indicate that the PPSP is nearly Gaussian, adiabatic, nearly scale invariant and weak in a sense that we will specify in the next section. These properties can be found in simple single-field models [9] but there is no particular reason to believe that the energy density during Inflation is dominated by a *single* field. Thus, a great deal of effort has been placed on studying the new effects that may appear as a signature of multi-field Inflation. In this work we will review tools sufficient to i) analyze multi-field Inflation, ii) compare it with observations and iii) compare its predictions with those of single-field Inflation.

Arguably, the strongest candidate for a theory of Quantum Gravity available is Superstring Theory. According to the theory, the fundamental constituents of the Universe are one-dimensional objects known as strings, whose length, l_s , is slightly above the Planck length ($\sim 10^{-33}$ cm). In order for the theory to be anomaly free they need to live in a 10-dimensional manifold. Six of these dimensions are usually assumed to be compact and small enough to have avoided detection so far. Often, as a byproduct of this process of compactification, we end up with the so-called *moduli*: scalar fields which parameterize the size and the shape of the compact dimensions. These moduli are massless at the classical level and in the absence of background *fluxes*. They are usually unstable, since their potential is so flat that their vacuum expectation values can become arbitrarily large. In this case, if they parameterize the size of the compact dimensions then the compact space would decompactify dynamically, and we would have been able to observe the extra dimensions. Thus, they are problematic and one is usually forced to introduce

additional sources of potential energy in the compact space (such as *orientifold planes*, fluxes or *Dp-branes*) to keep them fixed at a certain value.

Obtaining reasonable inflationary models from String Theory is a highly non-trivial task which we shall briefly review in section 5. The fundamental energy scale in String Theory is given by the inverse of the string length: $M_s = l_s^{-1}$. If the scale of Inflation, which is determined by the Hubble constant H , was placed near this energy scale, knowledge of the full dynamics of String Theory would be essential to describe it. Unfortunately, quantitative analysis of such a regime of Inflation is out of reach at present [23]. For this reason, most of the models developed so far are obtained by taking the so-called supergravity limit $E \ll M_s$ of the Superstring Theory, where E is the characteristic energy scale of the effective theory, $E = H$ for Inflation.

After integrating out the ultraviolet degrees of freedom, incorporating the effects of fluxes, localized sources and quantum corrections to the action, one generally arrives at a complicated effective Lagrangian describing the different moduli. Although a subset of the moduli may acquire large masses $m_{\text{mod}} \gg H$, which renders them dynamically frozen, a common outcome is that a significant number of moduli have masses $m_{\text{mod}} \lesssim H$, and are therefore dynamically active during Inflation. We recover the single field case when all the moduli have very large masses except the inflaton. Since the predictions of single-field Inflation are in agreement with observations, one is usually interested in studying multi-field scenarios where the inflaton is surrounded by a few other weakly interacting scalar fields. In this way the models are able to agree with observations and still include multi-field effects. These scenarios appear when the masses of all moduli satisfy $m_{\text{mod}} \gg H$.

From the last two paragraphs we see that the following hierarchy of energies is required: $M_s \gg m_{\text{mod}} \gg H$. Obtaining this hierarchy is probably the biggest challenge in String Inflation. The process of model building can be divided into two main tasks: 1) determining the effective Lagrangian and 2) computing the cosmological observables. In this thesis we will take up the second task. In particular, we will consider the toy model introduced in [8] and study its cosmological signatures in detail for the first time. In this reference, the corrections to the non-perturbative term in the superpotential, which appear through the gauge-kinetic function were presented for the first time.

The main goals of this project are:

- To review the tools necessary to study multi-field Inflation.
- To provide an introduction to model building in String Inflation, giving an overview of its major challenges.
- To study in detail for the first time the corrections introduced in the model in [8]. This includes understanding the effects of the different parameters in the cosmological observables and comparing with observations.

The structure of the thesis is as follows. In section 2 we include the basic knowledge of cosmology and single-field Inflation. In section 3 we present in some detail the basics of multi-field Inflation, with special attention to the two-field case, which is the main focus of this work. We test our code with some examples from the literature and comment on the multi-field effects that can arise as a result of the coupling between curvature and isocurvature. Many of the equations obtained here are simple generalizations of the ones developed in section 2. In section 4 we introduce the basics of String Theory and in section 5 we give an overview of model building in String Inflation. In section 6 we introduce the model presented in [8], and explain which are its innovative aspects. Then we solve numerically the dynamics of the model and use data from cosmological observations to test it. Finally, we draw our conclusions in section 7.

2 Cosmology

2.1 The Standard Model of Cosmology

As mentioned in the introduction, our Universe is well described by a flat FLRW metric:

$$ds^2 = a^2(\eta) [d\eta^2 - dx^2 - dy^2 - dz^2], \quad (1)$$

where η denotes conformal time, related to the usual coordinate time by $ad\eta = dt$.

In this work we use the conventions and notation from Ref. [20, 24]. In particular, we use natural units and set the reduced Planck mass to unity: $M_{\text{pl}} = (8\pi G)^{1/2} = 1$. Moreover, we denote derivatives with respect to the coordinate time with a dot and with respect to the conformal time with a prime. According to the Einstein equations of GR the scale factor must verify the following Friedmann equations:

$$H^2 = \frac{\rho}{3}, \quad (2)$$

$$\frac{\ddot{a}}{a} = -\frac{2}{3}(\rho + p), \quad (3)$$

where we have introduced the Hubble parameter $H \equiv \frac{\dot{a}}{a}$. Matter is introduced through the energy-momentum tensor, which is parameterized by the energy density ρ and the pressure p . They are usually related by an equation of state of the form $p = w\rho$, in which case the solution is

$$H = H_0 a^{-\frac{3}{2}(1+w)}, \quad (4)$$

where H_0 is the Hubble constant today. Defining the conformal-time version of the Hubble constant $\mathcal{H} \equiv \frac{a'}{a} = aH$, we can re-write the Friedmann equations using conformal time:

$$\mathcal{H}^2 = a^2 \frac{\rho}{3}, \quad (5)$$

$$\mathcal{H}^2 - \mathcal{H}' = \frac{1}{2}a^2(\rho + p). \quad (6)$$

2.2 The inflationary paradigm

During Inflation, instead of the usual time coordinate t , it is very convenient to use either conformal time or N_e , the number of e -foldings the scale factor grows until the end of Inflation,

$$N_e = \ln \frac{a(t_{\text{end}})}{a(t)}. \quad (7)$$

Inflation may be defined by the following equivalent conditions [22]

$$\ddot{a} > 0, \tag{8}$$

$$\epsilon < 1, \tag{9}$$

$$w < -\frac{1}{3}, \tag{10}$$

$$\frac{d}{dt} (aH)^{-1} < 0, \tag{11}$$

$$\frac{d \ln \rho}{d \ln a} < 1, \tag{12}$$

where we have introduced the parameter

$$\epsilon \equiv -\frac{\dot{H}}{H^2}. \tag{13}$$

The first condition simply says that the Universe is going through an accelerated expansion. The second one tells us that H is approximately constant, which means the scale factor a increases more or less like an exponential. The third one enables us to learn something about conformal time using Eq. (4):

$$\begin{aligned} \eta - \eta_i &= \int_{t_i=0}^t \frac{dt'}{a(t')} = \int_{a_i=0}^a \frac{da'}{H(t')a^2(t')} = \int_{a_i=0}^a a^{\frac{1}{2}(-1+3w)} da' \\ &= \frac{2}{H_0(1+3w)} a^{\frac{1}{2}(1+3w)} = \frac{2}{(1+3w)} \frac{1}{a(t)H(t)}. \end{aligned} \tag{14}$$

Note that in our units conformal time is the same as the comoving particle horizon. It is often the case that $w \simeq -1$, so that $\eta \simeq \frac{-1}{a(t)H(t)} = \frac{-1}{\mathcal{H}}$. The important quantity for solving the homogeneity problem is the comoving Hubble radius \mathcal{H}^{-1} , which tells us the maximum distance at which two particles can still have a non-negligible causal interaction. This is because \mathcal{H}^{-1} is roughly the time the scale factor needs to change significantly. We have just seen that the comoving Hubble radius and the comoving particle horizon are very similar during Inflation. Condition (11) tells us that both were larger in the past. This means that causally disconnected regions were in causal contact in the past. In this way Inflation solves the homogeneity problem. It can be shown [22] that to solve the flatness problem one needs at least around 60 e -foldings. Finally, the last condition tells us that the energy density is almost constant during Inflation.

These conditions can be satisfied if matter is described through N scalar fields φ^a , where $a = 1, 2, \dots, N$. In the particular case of a single Klein-Gordon field in a potential V the equations

of motion are:

$$\varphi'' + 2\mathcal{H}\varphi' + a^2V_\varphi = 0 \quad (15)$$

$$\mathcal{H} - \frac{1}{3} \left[\frac{1}{2}\varphi'^2 + a^2V_\varphi \right] = 0 \quad (16)$$

$$\mathcal{H}^2 - \mathcal{H}' - \frac{\varphi'^2}{2} = 0. \quad (17)$$

We refer to them as *background* equations since later we will introduce space-time dependent perturbations and only the unperturbed quantities will follow them. The energy-momentum tensor is given by:

$$T_0^0 = \rho, \quad T_i^0 = 0, \quad T_j^i = -p\delta_j^i, \quad (18)$$

with

$$\rho = \frac{1}{2}\partial^\mu\varphi\partial_\mu\varphi + V(\varphi), \quad (19)$$

$$p = \frac{1}{2}\partial^\mu\varphi\partial_\mu\varphi - V(\varphi). \quad (20)$$

Using these equations we see that w is given by:

$$w = \frac{p}{\rho} = \frac{\frac{1}{2}\partial^\mu\varphi\partial_\mu\varphi - V(\varphi)}{\frac{1}{2}\partial^\mu\varphi\partial_\mu\varphi + V(\varphi)}. \quad (21)$$

Since our Universe is homogeneous and isotropic to leading order, the unperturbed field does not depend on spatial coordinates. Furthermore, we are often allowed to use the slow-roll approximation $\ddot{\varphi} \ll 3H\dot{\varphi}$, $\dot{\varphi}^2 \ll 2V(\varphi)$ and in this case $w \approx -1$.

2.3 Cosmological perturbation theory

We have discussed that Inflation is so alluring not only because it solves the homogeneity problem but also because it provides a mechanism to generate the primordial inhomogeneities required for structure formation. To obtain the equations for the perturbed metric and the perturbed scalar fields one needs Cosmological Perturbation Theory. The most general perturbation of our physical system is given by:

$$ds^2 = a^2(\eta) \left\{ (1 + 2\phi) d\eta^2 + 2B_i d\eta dx^i - ((1 + 2D)\delta_{ij} + 2E_{ij}) dx^i dx^j \right\} \quad (22)$$

$$\varphi^a(\vec{x}, \eta) = \overline{\varphi^a}(\eta) + \delta\varphi^a(\vec{x}, \eta). \quad (23)$$

In the single-field case, the equation for the background field $\overline{\varphi}$ and for the scale factor $a(t)$ (unperturbed FLRW metric) are still given by Eq. (15). The equations for the perturbed

variables are more difficult since we need to perturb Eq. (15), Einstein equations and collect first-order terms. First of all, note that the metric can be re-written as:

$$ds^2 = a^2(\eta) \left[(1 + 2\phi) d\eta^2 + 2(\partial_i B + S_i) d\eta dx^i - [(1 + 2\psi) \delta_{ij} + 2\partial_{ij} E + 2\partial_{(i} F_{j)} + h_{ij}] dx^i dx^j \right], \quad (24)$$

with $\partial^i F_i = 0$, $\partial^i S_i = 0$, $\partial^i h_{ij} = 0$ and $h^i_i = 0$. The perturbations can be classified using the SO(3) symmetry of the background metric in: tensor perturbations (h_{ij} is divergenceless and traceless), vector perturbations (F_i, S_i are divergenceless) and scalar perturbations (ϕ, ψ, B and E). This decomposition is useful since the equations decouple for first order scalar, tensor and vector perturbations.

Not all of these perturbations are meaningful since, for example, perturbations in one coordinate system can disappear in another. There are two possible ways to proceed: one can either fix a gauge or use only gauge-invariant quantities and work in any gauge one wants. One useful choice [20, 24] for the gauge invariant quantities is: h_{ij} (the tensor perturbations are already gauge invariant) and

$$\Phi = \delta\phi - \frac{1}{a} [a(B - E)'] \quad (25)$$

$$\Psi = \delta\psi + \frac{a'}{a} (B - E) \quad (26)$$

$$\bar{V}_i = S_i - F'_i. \quad (27)$$

This means that only two of the scalar perturbations and two of the vector perturbations were physical. We only need to consider the scalar perturbations Φ and Ψ (known as Bardeen potentials) and the tensor perturbations (gravitational waves) h_{ij} , since the vector perturbations decay very fast during Inflation and we can forget about them. The most common choice in inflationary model building is to use the Newtonian Gauge $E = B = 0$. This is the one used in our main references for multi-field Inflation and it is the one we shall use. In this gauge the scalar metric perturbations coincide with the gauge-invariant Bardeen potentials. Note, however, that for the standard Big Bang Evolution it is more frequent to use the Synchronus Gauge.

In this work we are only concerned with first order perturbation theory. Our next step is to introduce the perturbations in the scalar fields and the metric in the Einstein equations. This is a rather laborious task, since one needs to perturb both the energy-momentum tensor of the scalar fields and the Einstein tensor, but it presents no conceptual difficulty. One can show that, because we are only interested in the first-order perturbations, the equations decouple for scalar, tensor and vector perturbations. The final result of this process [20, 24] is, separating also the scalar and tensor parts of an arbitrary energy-momentum tensor:

- Scalar equations:

$$(00) \quad \nabla\Psi - 3\mathcal{H}(\Psi' + \mathcal{H}\Phi) = \frac{a^2}{2}\delta T_0^0 \quad (28)$$

$$(0i) \quad \partial_i(\Psi' + \mathcal{H}) = \frac{a^2}{2}\delta T_i^0 \quad (29)$$

$$(ij) \quad \left\{ \Psi'' + \mathcal{H}(2\Psi + \Phi)' + (2\mathcal{H}' + \mathcal{H}^2)\Phi \right. \quad (30)$$

$$\left. + \frac{1}{2}\nabla^2(\Phi - \Psi) \right\} \delta_j^i + (\partial^i \partial_j - \frac{1}{2}\delta_j^i)(\Phi - \Psi) = \frac{-a^2}{2}\delta T_j^i \quad (31)$$

- Tensor equation:

$$h''_{ij} + 2\mathcal{H}h'_{ij} - \nabla^2 h_{ij} = 2a^2\delta T_j^i \quad (32)$$

2.4 Single-field Inflation

2.4.1 Classical theory

We denote with an over-line the unperturbed quantities. We consider a single Klein-Gordon field:

$$S = \int d^4x \sqrt{-g} \left\{ \frac{R}{2} - \frac{1}{2}g^{\mu\nu} \partial_\mu \varphi \partial_\nu \varphi - V(\varphi) \right\}. \quad (33)$$

Introducing the so-called Mukhanov-Sasaki variable $v \equiv a\delta\varphi + z\phi$, with $z \equiv \frac{a\bar{\varphi}}{\mathcal{H}}$, the classical equations can be simplified to the so-called Mukhanov-Sasaki equations:

- Scalar equations:

$$v'' - \nabla^2 v - \frac{z''}{z}v = 0 \quad (34)$$

$$\nabla^2 \phi = \frac{1}{2} \frac{\mathcal{H}}{a^2} (zv' - z'v). \quad (35)$$

- Tensor equations for a symmetric, transverse and traceless polarization tensor $e_{ij}(\vec{k}, \lambda)$ such that $e_{ij}(-\vec{k}, \lambda) = e_{ij}^*(\vec{k}, \lambda)$, $\sum_\lambda e_{ij}^*(\vec{k}, \lambda)e^{ij}(\vec{k}, \lambda) = 4$, $h_{ij} = he_{ij}$ and $\nu \equiv \frac{1}{\sqrt{2}}h$:

$$\nu'' - \nabla^2 \nu - \frac{a''}{a}\nu = 0. \quad (36)$$

It is useful to consider these equations in Fourier space. We denote the Fourier transform with a subscript k . Taking the far future limit in Eq. (34), when the scale is far outside the horizon, $\nabla^2 \sim -k^2$ and $k \ll aH = \mathcal{H}$, the k term is negligible and the non-decaying solution is $v \propto z$.

This suggests using a different quantity, known as the perturbation in the curvature of comoving surfaces $\mathcal{R}_k = -\phi_k - H \frac{\delta\varphi_k}{\dot{\varphi}} = -\frac{v_k}{z}$, which in this limit is constant: it does not evolve outside the horizon. Since during Inflation the comoving Hubble radius aH is decreasing, all scales except the very large ones (small k) eventually exit the horizon ($k = aH$). During the standard Big Bang theory, the Hubble radius increases, so these scales eventually enter the horizon. The key property we have just derived enables us to set initial conditions for the perturbations when they enter the horizon. We have a mapping between Inflation and observations, which is not affected by the unknown physics in between (such as the Reheating epoch).

2.4.2 Quantum theory

The next step is to canonically quantize the perturbations. This is done in very similar ways for scalar and tensor perturbations, whose Mukhanov-Sasaki equation differ only by $z \longleftrightarrow a$, $v \longleftrightarrow \nu$. Thus, we will do it only for the scalar perturbations. First we promote the classical variables to quantum field operators and impose canonical commutation relations. The conjugate momentum is given by $\hat{\pi} = \hat{v}'$. The expansion of the field operator in terms of creation and annihilation operator is:

$$\hat{v}(\eta, \vec{x}) = \int \frac{d^3k}{(2\pi)^3} \left[v(\vec{k}, \eta) e^{i\vec{k}\vec{x}} \hat{a}(\vec{k}) + v^*(\vec{k}, \eta) e^{-i\vec{k}\vec{x}} \hat{a}^\dagger(\vec{k}) \right], \quad (37)$$

and the commutation relations read:

$$[\hat{v}(\eta, \vec{x}), \hat{v}(\eta, \vec{x}')] = [\hat{\pi}(\eta, \vec{x}), \hat{\pi}(\eta, \vec{x}')] = 0 \quad (38)$$

$$[\hat{v}(\eta, \vec{x}), \hat{\pi}(\eta, \vec{x}')] = i\delta(\vec{x} - \vec{x}'). \quad (39)$$

We can neglect the vectorial nature of k since the Heisenberg equations for the fields, Eq. (34), depend only on its absolute value. The next step is to set initial conditions. As usual in QFT we use the Heisenberg picture, where the quantum states do not depend on time. The quantum state of the system is usually assumed to be the ground state, $|0\rangle$, such that: $a(\vec{k})|0\rangle = 0$ for all \vec{k} and $\langle 0|0\rangle = 1$. This state is often called the *Bunch-Davies* vacuum. Now, the quantities we want to compare with observations [9] are the Green Functions. In particular we will focus on the two-point correlation function:

$$\langle 0|\hat{\mathcal{R}}(\vec{x}, \eta)\hat{\mathcal{R}}(\vec{x}', \eta)|0\rangle = \frac{1}{z^2}\langle 0|\hat{v}(\vec{x}, \eta)\hat{v}(\vec{x}', \eta)|0\rangle = \frac{1}{z^2} \int \frac{d^3k}{(2\pi)^3} |v_k|^2 e^{i(\vec{k}-\vec{k}')\vec{x}}, \quad (40)$$

where we have used Eq. (37). Using Wick's theorem we can now see that, since we are computing vacuum expectation values, the classical random field we obtain is Gaussian [9]. Given a homogeneous and isotropic Gaussian random field $\mathcal{F}(\vec{x})$ whose k -dependent variance is σ_k , we

define the power spectra as: $P(k) = \frac{\sigma_k^2 k^3}{(2\pi)^2}$, so the two-point correlation function reads:

$$\langle \mathcal{F}(\vec{x}) \mathcal{F}(\vec{x}') \rangle = \int_0^\infty P(k) \frac{dk}{k}. \quad (41)$$

Comparing Eq. (41) and (40) we find that the power spectra, once the perturbations have become classical, are given by [20]:

$$P_{\mathcal{R}}(k, \eta) = \frac{k^3}{(2\pi)^2} \frac{|v_k|^2}{z^2}. \quad (42)$$

In parts of the literature their definition differ from ours by a factor of 1/2. We could obtain a similar expression for the power spectra of tensor perturbations $P_T(k, \eta)$. For simplicity we will not give the details here and refer the interested reader to ref [9, 20].

2.4.3 Cosmological observables

We have mentioned that the quantity we compare with experiments is the primordial power spectrum of perturbations (PPSP). In the case of single-field Inflation we only need to evaluate it at horizon exit, since it does not evolve later on. We need to do it for scales that exit the horizon between 50-60 e -foldings before the end of Inflation, since those are the ones relevant for observations. We now define the four experimental quantities that shall concern us. We also write the observational bounds from CMB and LSS observations [13, 14, 25], all with a 95% confidence level except the last one, with 68%. The tilt of the scalar power spectra is defined as:

$$n_s \equiv 1 + \frac{d \ln P_{\mathcal{R}}(k)}{d \ln k} = 0.968 \pm 0.006, \quad (43)$$

the running of the tilt

$$\frac{d n_s}{d \ln k} = -0.003 \pm 0.007, \quad (44)$$

the tensor-to-scalar ratio

$$r \equiv \frac{P_T(k)}{P_{\mathcal{R}}(k)} < 0.07, \quad (45)$$

and the amplitude of the scalar perturbations

$$A_s \equiv P_{\mathcal{R}}(k) = (2.207 \pm 0.076) \times 10^{-9}. \quad (46)$$

It is straightforward to compute these quantities once we have obtained the power spectra numerically. However, it is often the case in single-field Inflation that one can use the slow-roll approximation $\ddot{\varphi} \ll 3H\dot{\varphi}$, $\dot{\varphi}^2 \ll 2V(\varphi)$ to obtain analytical expressions for the cosmological

observables [10, 22]. We will use these expressions when we compare the multi-field and single-field predictions. In this slow-roll limit the parameters ϵ , $\eta_{SF} \equiv -\frac{\ddot{\phi}}{H\dot{\phi}}$, $\sigma \equiv \frac{\dot{\epsilon}}{\epsilon H}$, $\kappa \equiv \frac{\dot{\sigma}}{\sigma H}$ and $\xi = -\frac{\ddot{\phi}}{H\dot{\phi}}$ are very small. It can be shown that these parameters are not only small but also constant to a good approximation. The final formulas for the cosmological observables can be written in terms of the parameters, without solving the Mukhanov-Sasaki equation:

$$P_{\mathcal{R}}(k) = \frac{H^2}{8\pi\epsilon} \left(\frac{k}{aH} \right)^{n_s-1}, \quad (47)$$

$$n_s(k) = 1 - 2\epsilon - \sigma, \quad (48)$$

$$\frac{d n_s}{d \ln k}(k) = 2(\eta_{SF}\xi - \eta_{SF}^2 + 4\epsilon^2 - 11\eta_{SF}\epsilon), \quad (49)$$

$$r(k) = 16\epsilon_*, \quad (50)$$

where we have introduced the symbol $*$, which means the quantity evaluated at horizon crossing.

It will be useful to re-write the Mukhanov-Sasaki equation (34) in Fourier space and in terms of the slow-roll parameters. To do this we note that $z^2 = 2a^2\epsilon$, so that $\frac{z'}{z} = aH(1 + \frac{\sigma}{2})$. After computing z'' we obtain:

$$v_k'' + \left[k^2 - a^2 H^2 \left(2 - \epsilon + \frac{3\sigma}{2} - \frac{\epsilon\sigma}{2} + \frac{\sigma^2}{4} + \frac{\sigma\kappa}{2} \right) \right] v_k = 0 \quad (51)$$

If the slow-roll approximation is valid then we can neglect second-order terms in the last equation and, using $\sigma = 2(\epsilon - \eta_{SF})$, we arrive at:

$$v_k'' + \left[k^2 - \frac{1}{\eta^2} (2 + 6\epsilon - 3\eta_{SF}) \right] v_k = 0. \quad (52)$$

Finally, we shall remark that in any realistic model of Inflation the cosmological observables barely depend on the initial conditions of the scalar fields. This is because the background equations show a strong attractor behaviour. The attractor solution is known as the slow-roll attractor.

3 Multi-field Inflation

3.1 Classical theory

In this work we consider actions for several scalar fields with minimal coupling to gravity:

$$S = \int d^4x \sqrt{-g} \left\{ \frac{R}{2} - \frac{1}{2} g^{\mu\nu}(x) \gamma_{ab}(\varphi) \partial_\mu \varphi^a \partial_\nu \varphi^b - V(\varphi) \right\}. \quad (53)$$

We have introduced the metric γ on the manifold \mathcal{M} spanned by the scalar fields. Note Eq. (53) is the multi-field generalization of Eq. (33). The scalar fields may be thought of as coordinates in this manifold, with Christoffel symbols given by

$$\Gamma_{bc}^a = \frac{1}{2} \gamma^{ad} (\partial_b \gamma_{dc} + \partial_c \gamma_{bd} - \partial_d \gamma_{bc}) \quad (54)$$

and the Riemann tensor by

$$\mathbb{R}_{bcd}^a = \partial_c \Gamma_{bd}^a - \partial_d \Gamma_{bc}^a + \Gamma_{ce}^a \Gamma_{db}^e - \Gamma_{de}^a \Gamma_{cb}^e. \quad (55)$$

In the cases that are of interest here, it can be shown that the dynamics for the tensor perturbations is very well approximated by the slow-roll, single-field formulas introduced before, with a simple modification that we will explain later. For this reason we only need to study the full dynamics of the scalar perturbations. The only changes between the SF and the MF case are:

- i) The Background Equation for the scalar fields is no longer the Klein-Gordon equation, but:

$$\ddot{\varphi}^a + \Gamma_{bc}^a \dot{\varphi}^b \dot{\varphi}^c + 3H \dot{\varphi}^a + \gamma^{ab} \frac{\partial V}{\partial \varphi^b} = 0. \quad (56)$$

Also, introducing $|\dot{\varphi}|^2 = \gamma_{ab} \dot{\varphi}^a \dot{\varphi}^b$, the Friedmann equations now read:

$$H^2 = \frac{1}{3} \left(\frac{a^2 |\dot{\varphi}|'^2}{2} + V \right) \quad (57)$$

$$\mathcal{H}^2 - \mathcal{H}' = \frac{|\dot{\varphi}|'^2}{2}. \quad (58)$$

- ii) The expression for the energy-momentum tensor is more complicated. This means more algebra is needed to compute its perturbation and introduce them in Eq. (29).

- iii) The final equations for the perturbations are more complicated. For simplicity, the most studied case in the literature is the two-field case. In this case one can decompose the perturbations in two directions: Tangent (\parallel) or Normal (\perp) to the background trajectory. These two

directions are determined by the two component vectors:

$$T = \frac{1}{|\dot{\bar{\varphi}}|} \left(\dot{\bar{\varphi}}^1, \dot{\bar{\varphi}}^2 \right) \quad (59)$$

$$N = \frac{1}{|\dot{\bar{\varphi}}|\sqrt{\gamma}} \left(-\gamma_{22}\dot{\bar{\varphi}}^2 - \gamma_{12}\dot{\bar{\varphi}}^1, \gamma_{11}\dot{\bar{\varphi}}^1 + \gamma_{21}\dot{\bar{\varphi}}^2 \right), \quad (60)$$

where we have introduced the determinant of the metric in field space γ . We will see that this decomposition is useful since the perturbation along the tangent direction reduces to the single-field perturbation in certain limits. There are now two Mukhanov-Sasaki variables:

$$Q^a = \delta\varphi^a + \frac{\dot{\bar{\varphi}}^a \phi}{H} \quad a = 1, 2. \quad (61)$$

For convenience we multiply them by the scale factor and project them along the tangent and normal directions. The coordinates of the vector aQ in the basis $\mathcal{B} = \{T, N\}$ then read:

$$aQ \equiv (v, u) = a(T_a Q^a, N_a Q^a). \quad (62)$$

The first-order equations for the two gauge-invariant perturbations $v^a = (v, u)$ (they will correspond to curvature and isocurvature perturbations) are:

$$v'' + 2\zeta u' - \zeta^2 v + \zeta' u + k^2 v + \Omega_{11} v + \Omega_{12} u = 0, \quad (63)$$

$$u'' - 2\zeta v' - \zeta^2 u - \zeta' v + k^2 u + \Omega_{21} v + \Omega_{22} u = 0, \quad (64)$$

where

$$\zeta = aH\eta_{\perp}, \quad (65)$$

$$\Omega_{11} = -a^2 H^2 (2 + 2\epsilon - 3\eta_{\parallel} + \eta_{\parallel}\xi_{\parallel} - 4\epsilon\eta_{\parallel} + 2\epsilon^2 - \eta_{\perp}^2), \quad (66)$$

$$\Omega_{12} = \Omega_{21} = a^2 H^2 \eta_{\perp} (3 + \epsilon - 2\eta_{\parallel} - \xi_{\perp}), \quad (67)$$

$$\Omega_{22} = -a^2 H^2 (2 - \epsilon) + a^2 M^2 \quad (68)$$

and

$$M^2 = V_{NN} + H^2 \epsilon \mathbb{R}, \quad \mathbb{R} = TN^b T^c N^d \mathbb{R}_{abcd}, \quad (69)$$

$$V_{NN} = N^a N^b D_b V_a, \quad D_b V_a \equiv \frac{\partial}{\partial \bar{\varphi}^b} \frac{\partial V}{\partial \bar{\varphi}^a} - \Gamma_{bc}^a \frac{\partial V}{\partial \bar{\varphi}^c}, \quad (70)$$

where we have introduced the following parameters:

$$\epsilon \equiv -\frac{\dot{H}}{H^2} = \frac{|\dot{\bar{\varphi}}|^2}{2H^2}, \quad (71)$$

which is the multi-field generalization of Eq. (13), and

$$\eta_{\parallel} \equiv -\frac{|\ddot{\varphi}|}{H|\dot{\varphi}|}, \quad \eta_{\perp} \equiv \frac{N^a \partial_a V}{H|\dot{\varphi}|}, \quad (72)$$

$$\xi_{\parallel} \equiv -\frac{|\ddot{\varphi}|}{H|\dot{\varphi}|}, \quad \xi_{\perp} \equiv -\frac{\dot{\eta}_{\perp}}{H\eta_{\perp}}. \quad (73)$$

Eq. (63) is the generalization of the single-field Eq. (34). Note that the equation is already in Fourier space and that we are dropping the k -dependence in the subscripts of u and v . In section 2.5 we defined a set of parameters which were useful in single-field Inflation. It should be clear that their multi-field generalization is given by the parameters ϵ , η_{\parallel} and ξ_{\parallel} . The key property of the single-field perturbation v_{SF} is that it is proportional to z far outside the horizon, which means that \mathcal{R} tends to a constant. In general, this property does not appear in the two-field case, due to the coupling between curvature and isocurvature, which can cause evolution far outside the horizon. This coupling is controlled by the parameter η_{\perp} , which appears in Ω_{11} , Ω_{12} and ζ . The parameter η_{\perp} has a simple geometrical interpretation: it measures the amount of bending of the trajectory in field space. To be more precise, it can be written as $|\eta_{\perp}| = \frac{|\ddot{\varphi}|}{H} \kappa^{-1}$, where κ is the radius of curvature of the trajectory in field space [26]. We can learn something about these complicated equations by taking the so-called single-field, decoupling or weak-coupling limit $\eta_{\perp} \rightarrow 0$. If we identify η_{SF} with η_{\parallel} , and notice that $\sigma = 2(\epsilon - \eta_{\parallel})$ and $\frac{\sigma\kappa}{2} = 2\epsilon^2 - \eta_{\parallel}^2 - 3\epsilon\eta_{\parallel} + \eta_{\parallel}\xi_{\parallel}$, then taking $\eta_{\perp} = 0$ in Eq. (63) we recover Eq. (51). This means that in the decoupling limit the curvature perturbations are frozen on superhorizon scales, as in the single-field case, while the isocurvature perturbations decay rapidly [27]. If we are also in the slow-roll regime, then the equations reduce to:

$$v'' + \left\{ k^2 + \frac{1}{\eta^2} (-2 - 6\epsilon + 3\eta_{\parallel}) \right\} v = 0 \quad (74)$$

$$u'' + \left\{ k^2 + \frac{1}{\eta^2} \left(-2 + \frac{M^2}{H^2} + \left(-3 + \frac{2M^2}{H^2} \right) \epsilon \right) \right\} u = 0. \quad (75)$$

The corresponding single-field equation for the curvature perturbation is Eq. (52).

3.2 Quantum theory

As in the single-field case, we expand the perturbations as a sum of Fourier modes:

$$\hat{v}^a(\eta, \vec{x}) = \int \frac{d^3k}{(2\pi)^3} \sum_{\alpha} \left[v_{\alpha}^a(\vec{k}, \eta) e^{i\vec{k}\vec{x}} \hat{a}_{\alpha}(\vec{k}) + v_{\alpha}^{a*}(\vec{k}, \eta) \right] e^{-i\vec{k}\vec{x}} \hat{a}_{\alpha}^{\dagger}(\vec{k}). \quad (76)$$

The index $a = 1, 2$ runs over the two perturbations while the index $\alpha = 1, 2$ runs over the number of independent solutions of the differential equation. Notice that there are two types of creation and annihilation operators, since there are two scalar quantum modes or independent solutions. The first solution $\alpha = 1$ is (v_1, u_1) and the second one is (v_2, u_2) . The directions T and N are not necessarily the same as the directions of the quantum modes. Since the solutions are linearly independent, both need to satisfy *independently* the classical MS equations:

$$v''_{\alpha} + 2\zeta u'_{\alpha} - \zeta^2 v_{\alpha} + \zeta' u_{\alpha} + k^2 v_{\alpha} + \Omega_{11} v_{\alpha} + \Omega_{12} u_{\alpha} = 0 \quad (77)$$

$$u''_{\alpha} - 2\zeta v'_{\alpha} - \zeta^2 u_{\alpha} - \zeta' v_{\alpha} + k^2 u_{\alpha} + \Omega_{21} v_{\alpha} + \Omega_{22} u_{\alpha} = 0. \quad (78)$$

Then we impose canonical commutation relations:

$$[\hat{v}^a(\eta, \vec{x}), \hat{v}^b(\eta, \vec{x}')] = [\hat{\pi}^a(\eta, \vec{x}), \hat{\pi}^b(\eta, \vec{x}')] = 0 \quad (79)$$

$$[\hat{v}^a(\eta, \vec{x}), \hat{\pi}^b(\eta, \vec{x}')] = i\delta^{ab}(\vec{x} - \vec{x}'). \quad (80)$$

Again, we work in the Heisenberg representation and choose as initial quantum state the ground state. It can be shown that in the limit when the scale is far inside the horizon [26] the equations of motion reduce to:

$$v''_{\alpha} + k^2 v_{\alpha} = 0 \quad (81)$$

$$u''_{\alpha} + k^2 u_{\alpha} = 0, \quad (82)$$

which means that in this limit there is no mixing between different α -modes. As explained in [26], appropriate initial conditions are then, for the two solutions:

$$v_1(k, \eta) = \frac{1}{\sqrt{2k}} e^{ik\eta} \quad u_1(k, \eta) = 0 \quad (83)$$

$$v_2(k, \eta) = 0 \quad u_2(k, \eta) = \frac{1}{\sqrt{2k}} e^{ik\eta}. \quad (84)$$

3.3 Cosmological observables

After solving the equations numerically one time for each set of initial conditions, we are ready to compute observables. As we anticipated v corresponds to the curvature and u to the isocurvature perturbation:

$$\mathcal{R} \equiv \frac{v}{z} = \frac{H}{a|\dot{\varphi}|} v \quad (85)$$

$$\mathcal{S} \equiv \frac{u}{z} = \frac{H}{a|\dot{\varphi}|} u. \quad (86)$$

Using the commutation relations of the ladder operators as we did in the single-field case, we find that:

$$\langle 0 | \hat{\mathcal{R}}(\vec{x}, \eta) \hat{\mathcal{R}}(\vec{x}', \eta) | 0 \rangle = \frac{1}{z^2} \langle 0 | \hat{v}(\vec{x}, \eta) \hat{v}^*(\vec{x}', \eta) | 0 \rangle = \frac{1}{z^2} \int \frac{d^3 k}{(2\pi)^3} \sum_{\alpha} |v_{\alpha}(k)|^2 e^{i(\vec{k} - \vec{k}') \cdot \vec{x}}. \quad (87)$$

This leads us to define the power spectra of each perturbation as:

$$P_{\mathcal{R}}(k, \eta) = \frac{k^3}{(2\pi)^2} \frac{1}{z^2} \sum_{\alpha} |v_{\alpha}(k)|^2 = \frac{k^3}{(2\pi)^2} \frac{1}{z^2} (|v_1(k)|^2 + |v_2(k)|^2) \quad (88)$$

$$P_S(k, \eta) = \frac{k^3}{(2\pi)^2} \frac{1}{z^2} \sum_{\alpha} |u_{\alpha}(k)|^2 = \frac{k^3}{(2\pi)^2} \frac{1}{z^2} (|u_1(k)|^2 + |u_2(k)|^2). \quad (89)$$

Since the perturbations are coupled, they can evolve after horizon exit. In general this can be a problem, since one would need to follow the evolution of both quantities all the way until the scale re-enters the horizon during radiation or matter domination. However, if by the end of Inflation the isocurvature perturbation has decayed fast enough- meaning that the system has reached the adiabatic limit- one can still use Weinberg's theorem [9, 22, 23]. Weinberg starts by proving that *whatever the constituents of the universe and the classical equations governing them may be*, these equations always have a physical solution for which \mathcal{R} approaches a non-zero constant \mathcal{R}_0 far outside the horizon. This solution is called the adiabatic mode. Then he shows that in single-field Inflation this solution is always excited. He then concludes that the curvature perturbations set up during single-field Inflation always remain conserved after Inflation. In the same way, the adiabatic limit can be reached in multi-field Inflation, and we can still make predictions. The only difference is that now we need to evaluate the curvature power spectra at the end of Inflation, or at least once the adiabatic limit has been reached.

3.4 Numerical example

In this section we will consider a simple two-field potential:

$$V(\varphi, \chi) = \frac{1}{2} m_{\varphi}^2 \varphi^2 + \frac{1}{2} m_{\chi}^2 \chi^2, \quad (90)$$

with canonical kinetic terms,

$$\gamma = \begin{pmatrix} 1 & 0 \\ 0 & 1 \end{pmatrix}. \quad (91)$$

This example shows the essence of multi-field effects which could appear in the more complicated potential we will consider in section 6, where they can be harder to study. We choose the parameters in the model as in [28]: $m_{\varphi} = 1.395 \times 10^{-6} M_{pl}$, $m_{\chi} = 7m_{\varphi}$, $\varphi_0 = \chi_0 = 12 M_{pl}$ and

the derivatives of the fields at their slow-roll values. In Fig. 1 we can see that the trajectory in field space turns around $N = 30$. As expected, this corresponds to a peak in η_{\perp} in Fig. 2. We can see in Fig. 3 that this causes super-horizon evolution. Before $N = 30$ both modes evolve independently. Then the isocurvature transfers its power to the curvature, and that is why the red curve decays very fast, while the black one enjoys a small bump. Therefore, it is only after $N = 30$ that the adiabatic regime is reached. Note that Fig. 3 reproduces the results from Fig. 1 in [28].

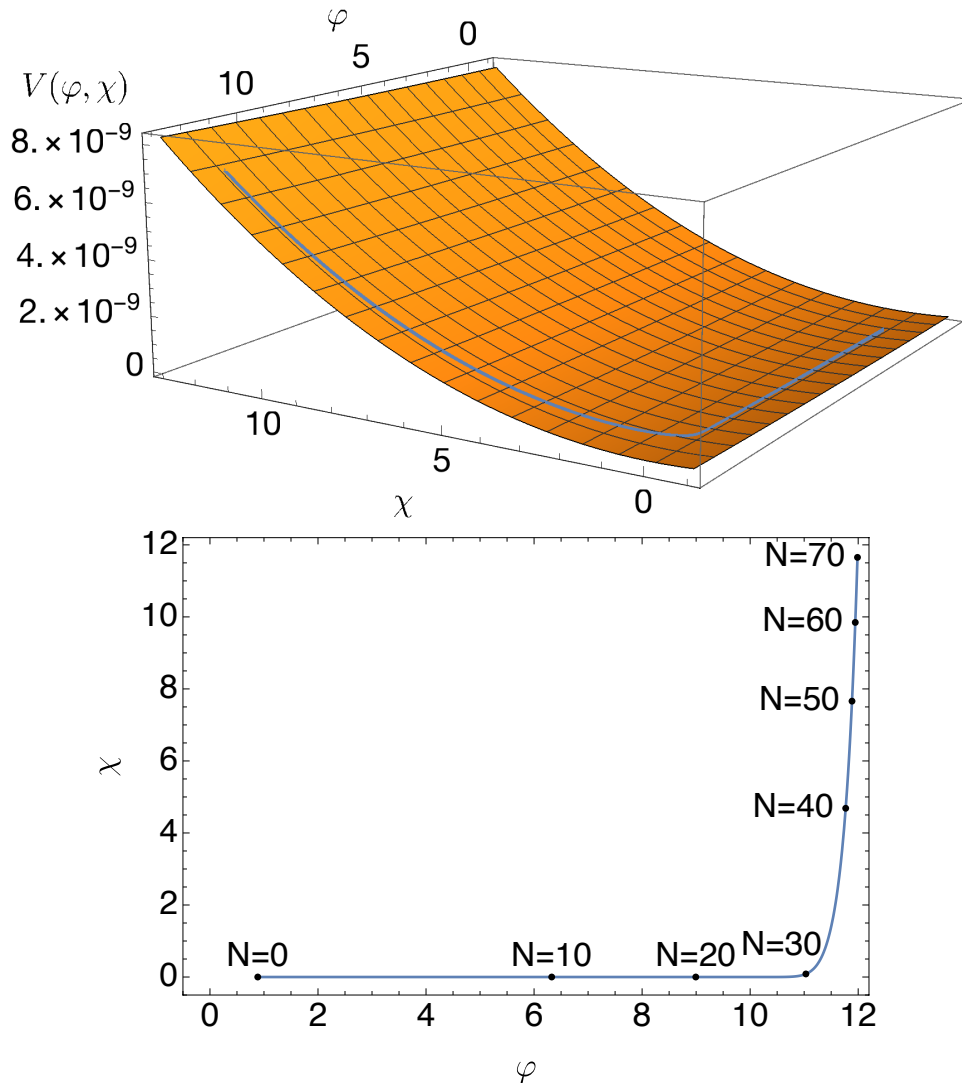


Figure 1: Potential and Trajectory in field space for the two-field square potential with parameters $m_{\varphi} = 1.395 \times 10^{-6} M_{\text{pl}}$, $m_{\chi} = 7m_{\varphi}$ and $\varphi_0 = \chi_0 = 12 M_{\text{pl}}$. We observe a sharp turn at $N = 30$, which is the cause of the coupling between curvature and isocurvature perturbations.

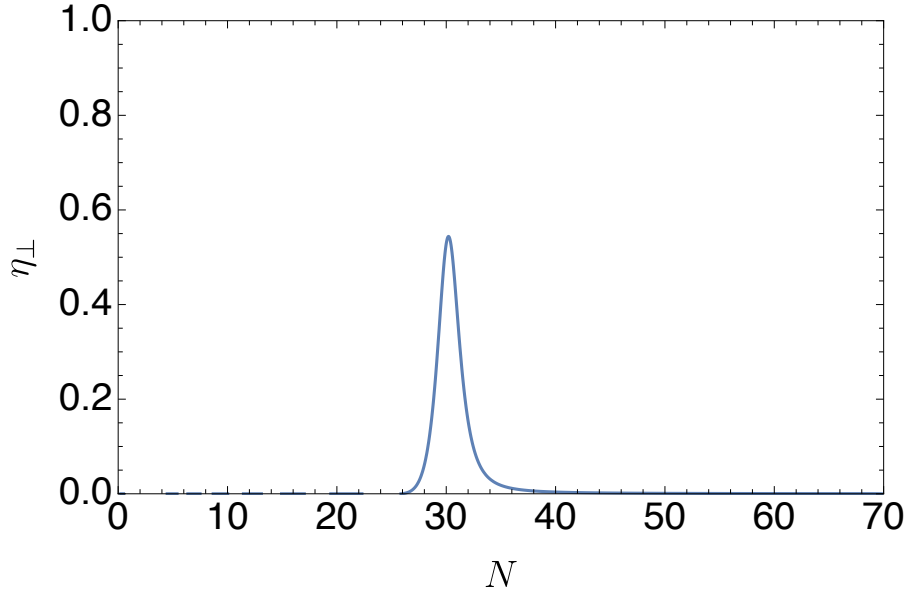


Figure 2: η_{\perp} for the two-field square potential with parameters $m_{\varphi} = 1.395 \times 10^{-6} M_{\text{pl}}$, $m_{\chi} = 7m_{\varphi}$ and $\varphi_0 = \chi_0 = 12 M_{\text{pl}}$.

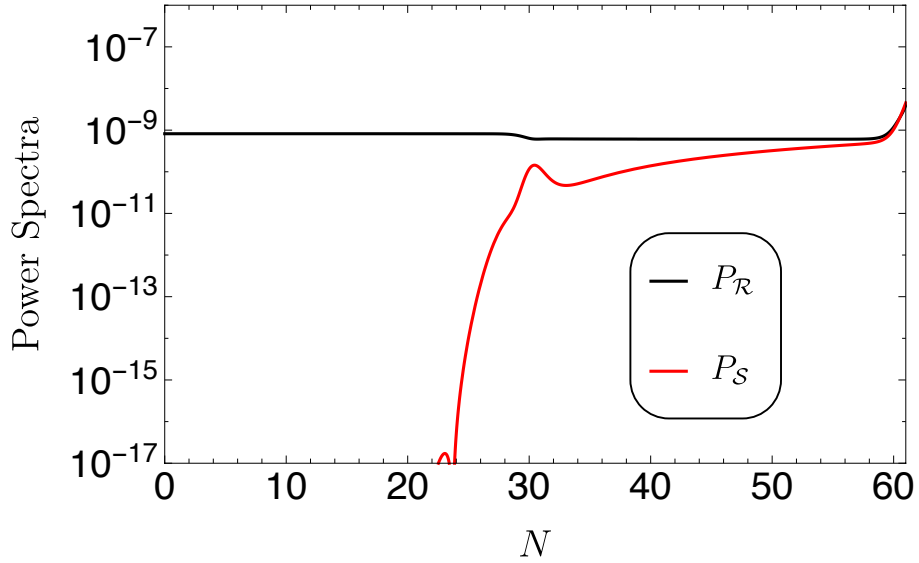


Figure 3: Power spectra for the scale that exits the horizon at $N = 60$ at the end of Inflation. $P_{\mathcal{R}}$ is given by Eq. (88) and $P_{\mathcal{S}}$ by Eq. (89). We can see a bump at $N = 30$, which corresponds to the peak in η_{\perp} in Fig. 2 and the turn in Fig. 1.

4 String Theory

4.1 Basics of String Theory

The fundamental objects of String Theory are no longer point particles, as in QFT, but one-dimensional objects known as *open* and *closed strings*. The SM particles appear then as a small set of the infinite vibrational modes of these strings. The *world-line* traced by the particles is replaced by the two-dimensional *worldsheet* traced by the string. The worldsheet can be parameterized by a finite spatial coordinate σ and a time coordinate τ . The coordinates of the string are defined as a mapping between the worldsheet and the target d -dimensional spacetime $x_M(\sigma, \tau)$ with $M = 0, 1, \dots, d - 1$. Interactions no longer occur at points, but are smeared out over spacetime in a smooth way. The length of the string l_s determines the energy scale of the massive excitations through $M_s \equiv (\alpha')^{-1/2} = l_s^{-1}$. It is the only renormalizable theory of Quantum Gravity known at present. In order to explain why the quantum version of General Relativity is non-renormalizable, String Theory must become effective before the Planck scale is reached, so we must have $M_s < M_{\text{pl}}$. String Theory is potentially able to incorporate all known forms of matter and interactions in a unified framework [29–31]. The theory is physically and mathematically consistent only after including supersymmetry and extra dimensions. Namely, a Supersymmetric String Theory (Superstring Theory) is anomaly free only if the number of dimensions is ten. With these conditions there are only five possible theories: Type I, Type IIA, Type IIB and the heterotic $E_8 \times E_8$ and $SO(32)$. We will only consider Type IIB in this work.

4.2 Type IIB Supergravity limit. Compactification. Moduli stabilization.

Type IIB String Theory is, at present, among the most promising theories to connect string theory with particle physics and cosmology, due to the presence, within its framework, of viable solutions both to stabilize moduli and to build local Standard Model-like constructions. We will shortly review how the four-dimensional effective theory is obtained from String Theory.

First of all, one starts by taking the low-energy limit of type IIB String Theory, $E \ll M_s$. In taking this limit we are ignoring massive string states and string loop effects. At this stage, one is able to write an action corresponding to a ten-dimensional type IIB supergravity, which has $\mathcal{N} = 2$ supersymmetries and whose field content is given by the massless degrees of freedom of the string. To go beyond this approximation one needs to include two types of corrections to the leading order action. Firstly, at leading order we are considering only tree diagrams for the strings. The perturbative expansion in the string loops is controlled by the string coupling

constant g_s . Secondly, there are α' corrections, which are related to the ten-dimensional supergravity equations themselves being only low-energy approximations to the full string theory. They count higher-order derivative terms. The parameter $\alpha' = M_s^{-2}$ controls this type of corrections since they appear in powers M_x/M_s , where M_x is an energy scale lower than the string scale.

Then, usually one assumes that space-time is a product of the form $\mathbb{R}^{3,1} \times X_6$, where X_6 is a six-dimensional Calabi-Yau manifold. It is often appropriate to take the further low-energy limit $E \ll M_{\text{KK}}$, where we have introduced the compactification scale M_{KK} (sometimes called M_c), whose inverse determines the size of the compact dimensions. In this limit one keeps only the zero-modes of the Kaluza-Klein tower, associated to each of the ten-dimensional states. One ends up in four-dimensional type IIB supergravity with $\mathcal{N} = 2$ supersymmetries. Finally, one takes an orientifold projection of the Calabi-Yau manifold to reduce the supersymmetries to $\mathcal{N} = 1$.

The bosonic part of the resulting $\mathcal{N} = 1$ low-energy four-dimensional Lagrangian can be displayed in the standard supergravity form [32], in terms of a *Kähler potential* K , a holomorphic *superpotential* W and a holomorphic *gauge-kinetic function* f_{ab} , where a, b run over the various vector multiplets, and I, J runs over all the different moduli:

$$\mathcal{L}_{\text{bos}} = \frac{M_{\text{pl}}^2}{2} R - \frac{1}{4} \text{Re}[f_{ab}(\Phi)] F_{\mu\nu}^a F^{b\mu\nu} - \frac{1}{4} \text{Im}[f_{ab}(\Phi)] F_{\mu\nu}^a \tilde{F}^{b\mu\nu} - K_{IJ} D_\mu \Phi^I D^\mu \bar{\Phi}^{\bar{J}} - V(\Phi^I, \bar{\Phi}^{\bar{J}}). \quad (92)$$

Here Φ^I are chiral superfields, but we will always understand that we are focusing on the lowest component $\Phi^I|_{\theta=0}$, so we can think of them as complex scalars. $F_{\mu\nu} F^{\mu\nu}$ is the usual term for the gauge bosons A_μ^a . Neither the gauge bosons nor the fermions in the theory play a role in this thesis. The F -term contribution to the supergravity scalar potential V is given in terms of K and W by:

$$V_F = e^{K/M_{\text{pl}}^2} \left\{ (K^{-1})^{I\bar{J}} D_I W D_{\bar{J}} \bar{W}^* - 3 \frac{|W|^2}{M_{\text{pl}}^2} \right\}, \quad (93)$$

where $K^{I\bar{J}}$ is the inverse of the Kähler metric $K_{I\bar{J}} = \frac{\partial}{\partial \Phi^I} \frac{\partial}{\partial \bar{\Phi}^{\bar{J}}} K(\Phi, \bar{\Phi})$ and the definition of the Kähler covariant derivative is:

$$D_I W = \partial_I W + \frac{1}{M_{\text{pl}}^2} (\partial_I K) W. \quad (94)$$

The D -term scalar potential reads:

$$V_D = \frac{1}{2} \text{Re}[f(\Phi)]^{-1 ab} D_a D_b, \quad (95)$$

where

$$D_a = \left[\frac{\partial}{\partial \Phi^I} W + \frac{1}{W} \frac{\partial}{\partial \Phi^I} W \right] (T_a)_{IJ} \Phi_J, \quad (96)$$

and T_a denote the gauge group generators. There are many different moduli that can appear in the resulting low-energy effective field theory. We will consider:

- Axio-dilaton modulus τ , whose vev gives the string coupling.
- Complex structure moduli ζ^a , which parameterize the shape of the extra dimensions.
- Kähler moduli T_i , which parameterize the size of the extra dimensions.
- Open string modulus Φ , which is associated with the position of a D-brane.

The source of the moduli problem is that in the absence of internal fluxes the superpotential vanishes [23], so only the Kähler potential contributes and the resulting potential is flat for all moduli: they are massless. In addition to the fundamental strings, String Theory contains other objects, like the so-called Dp -branes, which are hypersurfaces with p spatial dimensions and one time dimension, to which open strings can be attached. The D stands for Dirichlet, referring to the fact that open strings ending on a D-brane have Dirichlet boundary conditions in the directions perpendicular to the brane. Their endpoints cannot leave the D-brane. However, they have Neumann boundary conditions in the directions along the spatial dimensions, so the endpoints are free to move in the D-brane. Their presence introduces non-vanishing background fluxes, which contribute to the superpotential. In this way, by turning on background fluxes, both the dilaton and the complex structure moduli can be stabilized at tree level [33]. However, the part of the scalar potential which depends on the Kähler moduli, at tree level, usually goes as $V \sim 1/T^3$, so they can easily go to infinity. In this thesis we will assume that all moduli except the Kähler moduli have been stabilized in this way. Furthermore, we assume that their masses are very large compared to the typical energy scales of the remaining scalar fields, so that we can integrate them out at tree level. After integrating out the large massive moduli and ignoring irrelevant constants in the Kähler potential, one arrives at the following tree-level expressions for the Kähler potential and the superpotential, for the case of only one Kähler modulus:

$$K_{\text{tree}} = -3 \ln(T + \bar{T}), \quad (97)$$

$$W_{\text{tree}} = W_0, \quad (98)$$

where W_0 is a constant determined by the fluxes and the vacuum expectation values of the heavy moduli. It is known that in $\mathcal{N} = 1$ four-dimensional supergravity, the Kähler potential receives corrections at every order in perturbation theory. The gauge-kinetic function f also

receives corrections, but only at one-loop. However, the superpotential receives no corrections in perturbation theory. The superpotential is then only affected by non-perturbative corrections like those coming from instantons when D3 or D7-branes are present. The corrections therefore take the general form:

$$K = K_{\text{tree}} + K_{\text{p}} + K_{\text{np}}, \quad (99)$$

$$W = W_{\text{tree}} + W_{\text{np}}, \quad (100)$$

$$f = f_{\text{tree}} + f_{1L}. \quad (101)$$

It has been shown in the literature that these corrections can stabilize even all of the Kähler moduli. Most prominently, this can be achieved through terms in W_{np} , such that all the Kähler moduli are stabilized in a supersymmetric AdS vacuum [34]. This is often known as KKLT stabilization, the initials corresponding to the authors of [34]. The value of the potential in the post-inflationary vacuum is the value of the cosmological constant, measured to be close to zero, but positive. To match the observations it is necessary to "uplift" the Anti-de-Sitter solution (spacetime with negative curvature) to a Minkowski (flat spacetime) or tiny de Sitter (positive curvature) universe. For these reasons, it is useful to modify the system slightly, both to break supersymmetry and to raise the vacuum energy to zero or positive values. The idea is to do so in a way which does not ruin the success of the modulus stabilization just discussed. Following [34], the solution we will use in this thesis is to include a term of the form $V_{\text{up}} = e^K \Delta$ to the potential, where Δ is a constant parameter, which is tuned to obtain a Minkowski vacuum.

5 String Inflation

5.1 Motivation

In many well-known models, the scale of Inflation lies around 10^{15} GeV, which is relatively close to the scale of quantum gravity, the Planck scale $M_{pl} = (8\pi G)^{1/2} \approx 10^{18}$ GeV. It is then not unreasonable to assume that the physics behind Inflation will incorporate a quantum theory for gravity. At present, the theory which provides the best-developed and best-motivated framework of quantum gravity is String Theory. This makes it an appealing laboratory for seeking realistic inflationary models.

There are many other reasons why studying String Inflation is interesting. To begin with, it can provide a framework to answer questions such as those regarding the naturalness of Inflation. Inflationary models require relatively flat potentials and special initial conditions for the fields, and it is unclear how special these requirements actually are. String Theory could provide, in a natural way, flat potentials and the needed initial conditions for the fields. Another common motivation is that, by limiting ourselves to single-field inflation, we may be making unnecessary assumptions, and that by looking at Inflation from the String Theory point of view, many interesting new insights will arise naturally. For example, it is often assumed that the inflaton field remains a quantum state after inflation ends and still appears in the low-energy theory describing the later SMC epoch. However, if the inflaton were the separation between a brane and antibrane which mutually annihilate at the end of Inflation [35, 36], then the inflaton does not even make sense as a field in the later universe. Finally, arriving at a successful String Inflation model could pave the way for successful Reheating models, where one needs a strong coupling between the inflaton and the SM particles and a weak coupling between the inflaton and any other currently unobserved degree of freedom.

5.2 Energy scales and challenges in String Inflation

An ideal model of the early universe would include a theory of quantum gravity. Besides, it would use only fundamental topological data as input and, in the low-energy limit, one would be able to arrive at an effective field theory resembling the Standard Model via an explicit, well-controlled computation. Moreover, it would imprint distinctive signatures on the cosmological observables which would, of course, be consistent with current data, and would help us verifying the theory. Unfortunately, such a model is not expected to be available in the near future.

The most common approach to obtaining low-energy effective theories from String Theory was presented in the last section. There, we introduced two important energy scales: the string scale M_s and the compactification, Kaluza-Klein scale M_{KK} . Furthermore, we explained that

the following hierarchy is needed: $M_{\text{pl}} > M_s > M_{\text{KK}}$. Now, by Eq. (2) and Eq. (57), we know that the energy scale of Inflation is determined by the Hubble rate H . Applying what we have explained in section 4 we conclude that the complexity of an inflationary model in String Theory will depend crucially on how large H is, compared to M_s and M_{KK} :

- If $M_s \lesssim H$, then Inflation can only be studied using the whole apparatus of String Theory. Particles with masses $m \leq H$ can be produced, which correspond to nontrivial string excitation modes. As explained in section 4, this regime is out of reach at the moment.
- If $M_{\text{KK}} \ll H \ll M_s$, then we can use the ten-dimensional supergravity limit to study Inflation. In this regime all the extra-dimensional physics is important, the KK modes associated with the extra dimensions can be excited and it is still too difficult to work with.
- $H \ll M_{\text{KK}} \ll M_s$, then we can use all of the simplifications made in section 4, and study Inflation using the 4-dimensional supergravity limit. The biggest drawback of this regime is that most signatures from String Theory are highly suppressed, as far as CMB observables are concerned [23].

Of course, we will assume that Inflation falls in the last regime. The moduli stabilization problem introduced in section 4 is very relevant in String Inflation. To stabilize the moduli one needs to introduce new sources of potential energy, which can contribute to the inflaton potential. Therefore, one needs to study Inflation after all moduli have been stabilized. A simplifying assumption is that the masses we have given to most of the moduli are much larger than H and than the mass of the inflaton field $m_{\text{mod}} \gg m_\varphi, H$. In this case they can be integrated out and the inflationary action will involve only a few scalar fields. In this thesis we study the simplest case where there is only one companion to the inflaton field. We can summarize the hierarchy needed in string-inflationary models by:

$$H \ll m_{\text{mod}} \ll M_{\text{KK}} \ll M_s \ll M_{\text{pl}}. \quad (102)$$

At present, obtaining this hierarchy is probably the biggest challenge in String Inflation, since there is little room to accommodate all these energy scales. Keeping in mind the *ideal* features of a string inflationary model presented above, let us summarize the *essential* requirements that a successful model must meet [23]:

- The energy hierarchy in Eq. (102) must be realized, so that we can perform computations.
- The inflaton action should be computed in an expansion around a metastable de Sitter vacuum, with all approximations under control.

- For every string theory object we introduce to stabilize moduli, we must know the corresponding effect on the inflaton potential.
- The model needs to predict density fluctuations that are nearly scale-invariant, weak, Gaussian and adiabatic, in agreement with the current data for the cosmological observables, see Eq. (43-46).
- The inflationary phase must end and give way to a successful reheating of the Standard Model, without overproduction of relics.

6 Our Model

6.1 Motivation. Introducing one-loop corrections in W_{np} .

We will study a particular case within the general setup of sections 4 and 5, including type IIB String Theory with fluxes, orientifold and mobile D7-branes. Following [8], we consider toy models with a single Kähler modulus T , which parameterizes the volume of a four-cycle in the compact manifold Y_6 , and an inflaton multiplet Φ , which is the position modulus of a single mobile D7-brane, also wrapping a four-cycle. As in section 4, we assume that all other moduli have been given very large masses compared to the masses of T and Φ and that they have been integrated out. The three functions, to be obtained from String Theory, that define the four-dimensional supergravity are: the Kähler potential, the superpotential and the gauge-kinetic function. The precise form of the Kähler potential is not crucial for our discussion as long as it is shift-symmetric in the imaginary part of Φ , to guarantee enough flatness in the potential. It is not important because higher-order terms in K do not affect the leading-order terms in V that concern us here. Let us take the following ansatz for the Kähler potential:

$$K = -3 \ln (T + \bar{T}) + \frac{1}{2} (\Phi + \bar{\Phi})^2. \quad (103)$$

From Eq. (100) we know that W will be a sum of a constant term and a non-perturbative term. The possibility to use this non-perturbative term to stabilize T has been studied in the literature, where it was assumed to be of the form: $W = W_0 + A e^{-\alpha T}$, with α and A constant parameters. However, the one-loop corrections to the gauge-kinetic function in Eq. (101) can contribute to this non-perturbative term through [8]:

$$W = W_0 + \mu \Phi^2 + A e^{-f}, \quad (104)$$

$$f = \alpha T + \frac{1}{4\pi^2} \ln g(\Phi), \quad (105)$$

where μ is a constant and $g(\Phi)$ is a periodic function of Φ , containing the perturbative corrections to f . The constant piece of strength W_0 and the quadratic term for Φ , of mass μ , appear at tree level. The non-perturbative term which stabilizes T is the exponential, and it incorporates the one-loop corrections to the gauge-kinetic function. These corrections were studied for the first time in [8], where they were sourced by a gaugino condensate on a stack of $D7$ -branes. The different forms that this term can adopt are studied in this reference. In this thesis, we consider the following example:

$$W = W_0 + A [1 + \delta \sinh(\Gamma \Phi)] e^{-\alpha T} + \mu \Phi^2, \quad (106)$$

where δ and Γ are constant parameters and $\alpha = \frac{2\pi}{5}$. The amplitude of these corrections is determined by δ , and its frequency by Γ . The presence of the hyperbolic sine is determined by the details of the model. It is found by computing the Pfaffian of the one-loop diagram correcting the instanton action, which is a notoriously difficult task. Since the parameter δ is a one-loop coefficient, it should be smaller than 1. Typically, Γ^{-1} should correspond to the size of a four-cycle that is wrapped by a D7-brane. This size is, of course, bounded from above in the compact manifold. Its value depends on the explicit setup, but we always assume $\Gamma > 1$, again, see [8] for more details.

We are always working under the reasonable assumption that all other moduli, especially the complex structure and dilaton, have been stabilized at a high scale and play no role here. This will be the case if there is a separation of scales such that we can integrate them out at some higher scale. Then, in a specific example, μ would depend on the expectation values of the heavy fields; but we are not interested in the details of its origin. Further discussion on the details on the model can be found in [8] and references therein. The small size of the parameters W_0 and μ is related to the choice of fluxes, as explained in [7].

We obtain the scalar potential introducing Eq. (103) for K and Eq. (106) for W in Eqs. (93) and (95). At this stage, our Lagrangian is given by Eq. (92). The gauge bosons play no role, so we can forget about them. In section 4, we studied the general case, where a D-term appears if the theory has an Abelian gauge symmetry. By Eq. (95), the D-term is proportional to the charges of all the fields in the theory. In our case, there is no gauge symmetry, so the D-term potential vanishes. The bosonic Lagrangian then contains only the two complex scalar fields $I = (\Phi, T)$:

$$\mathcal{L}_{\text{bos}} = \frac{M_{\text{P}}^2}{2} R - K_{IJ} \partial_\mu \Phi^I \partial^\mu \bar{\Phi}^{\bar{J}} - V(\Phi^I, \Phi^{\bar{J}}). \quad (107)$$

We denote the four scalar fields inside the two complex fields by: $\Phi = \lambda + i\varphi$, $T = \tau + i\sigma$. It can be shown that the shape of the potential is such that the dynamics of λ and σ play no important role. This means that they can be integrated out at the origin. It can be seen that there is a stable AdS vacuum at $\varphi = 0$ and some value $\tau = \tau_0$. As explained in section 4, we must include an uplifting term in the potential of the form $V_{\text{up}} = e^K \Delta$, to tune the cosmological constant to a small, positive value. By demanding the existence of a Minkowski vacuum at $\varphi = 0$ we can eliminate the two parameters A and Δ in terms of the other parameters we have introduced plus τ_0 , which becomes a free parameter. We obtain:

$$A = \frac{6e^{\alpha\tau_0} W_0 (1 - \alpha\tau_0)}{3\Gamma^2 \delta^2 + 4\alpha\tau_0 (2 + \alpha\tau_0) - 6}, \quad (108)$$

$$\Delta = -\frac{2\sqrt{3}W_0 [(-1 + \alpha\tau_0) (3\Gamma^2\delta^2 (1 + \alpha\tau_0) + 4\alpha^2\tau_0^2(2 + \alpha\tau_0))]^{1/2}}{(-6 + 3\Gamma^2\delta^2 + \alpha\tau_0(2 + \alpha\tau_0))}. \quad (109)$$

Following [8] we take $\tau_0 = 10$. We have arrived at the final expression for our two-field (φ, τ) action, Eq. (53). Computing K_{IJ} and comparing Eq. (107) with Eq. (53) we obtain:

$$\gamma_{11} = 1 \quad (110)$$

$$\gamma_{22} = \frac{3}{(2\tau^2)} \quad (111)$$

$$\gamma_{i \neq j} = 0, \quad (112)$$

while for the scalar potential we obtain:

$$\begin{aligned} V(\varphi, \tau) = & \left\{ e^{-2\alpha\tau} 6W_0^2 (-1 + \alpha\tau_0) \right. \\ & \left[e^{2\alpha\tau} [3\Gamma^2\delta^2 (1 + \alpha\tau_0) + 4\alpha^2\tau_0^2 (2 + \alpha\tau_0)] + 3e^{2\alpha\tau_0}\Gamma^2\delta^2 (-1 + \alpha\tau_0) \cos\left(\frac{\Gamma^2\varphi^2}{2}\right) \right] \\ & - 12e^{2\alpha(\tau_0-\tau)}W_0^2\alpha(-1 + \alpha\tau_0)^2 \left(-2 - \delta^2 + \delta^2\cos\left(\sqrt{2}\Gamma\varphi\right)\right) \tau (3 + \alpha\tau) \\ & + \mu^2 (-6 + 3\Gamma^2\delta^2 + 4\alpha\tau_0 (2 + \alpha\tau_0))^2 \varphi^2 \\ & \left. - 6e^{\alpha(\tau_0-\tau)}W_0\alpha(-1 + \alpha\tau_0) (-6 + 3\Gamma^2\delta^2 + 4\alpha\tau_0 (2 + \alpha\tau_0)) \tau (2W_0 - \mu\varphi^2) \right\} \\ & / \left\{ 4(-6 + 3\Gamma^2\delta^2 + 4\alpha\tau_0 (2 + \alpha\tau_0))^2 \tau^3 \right\}. \quad (113) \end{aligned}$$

In our example the metric is simple enough to allow for a field re-definition $\tau \rightarrow \chi$ in such a way that both fields are canonically normalized ($\gamma_{ij} = \delta_{ij}$), at the expense of complicating (even more) our scalar potential. Only four of the parameters of the potential are relevant for the cosmological observables. The parameter W_0 can (and will) always be used to set the amplitude of the scalar perturbations equal to the experimental value. Both δ and Γ measure the strength of the oscillations induced in V by the corrections in the non-perturbative term of the superpotential. Γ also measures the frequency of these oscillations. Finally, the ratio $\frac{\mu}{W_0}$ (much less than unity), contributes to the flatness of the potential, and we will always tune it to match the observations as best as possible. Besides these parameters, we also need to choose the initial point for our trajectory, that is, initial conditions of the fields. If one chooses carelessly the initial values of the fields and their velocities, one typically observes very large initial oscillations of the fields around the attractor solution. Afterwards, the fields continue to roll down smoothly along the slow-roll solution. These oscillations always take place before the scales of cosmological interest enter the horizon ($N > 60$), so we can simply ignore them by setting the time derivatives of the fields equal to their slow-roll values right from the start.

W_0	W_0/μ	δ	Γ	φ_0	χ_0
0.006	290	0.096	1.31	15.2	2.91

Table 1: Set of parameters for small Γ and large δ .

6.2 Numerical evaluation

One of our goals is to study the signatures of the corrections we introduced in the superpotential, which appear as wavy modulations, parameterized by δ and Γ , in the potential, see Eq. (113). To put it simply, if these parameters are big enough, the scalar potential exhibits large and fast oscillations. In this case, we would expect our field trajectory to bend around the peaks in the potential, which would induce a large η_\perp and a large coupling between curvature and isocurvature. Therefore, we will try to search for this kind of behaviour. Depending on how large δ and Γ are, it will be useful to divide the parameter space in three different regimes, which we will now explore. For each regime, first, we will plot the potential and the trajectory in field space in the same figure, so that we can see if there are modulations in the potential that can lead to multi-field effects. Then, we solve numerically the Mukhanov-Sasaki equations, using *Mathematica*. We have explained that, since more than one scalar field is present, the curvature perturbation can, in principle, evolve outside the horizon. For this reason, we need to evolve the system until it reaches the adiabatic limit.

6.2.1 Small Γ and large δ

Let us begin with a comparably small value for Γ (remember that $\Gamma > 1$) and a value of δ chosen as large as allowed by the experimental bounds. In particular, we choose the set of parameters given in Table 1. In this case, since Γ is small, the frequency of the oscillations is small, as seen in Fig. 4. We can expect to observe multi-field effects only if η_\perp is as large as η_\parallel (which is of the order of 10^{-1}). In the present case we can see in Fig. 5 that η_\perp is really small, and would be negligible if plotted together with the rest of relevant parameters. Consequently, we are in the decoupling limit. It is easy to check that all the slow-roll parameters are small, so we expect the slow-roll, single-field formulas to match the numerical solutions quite well.

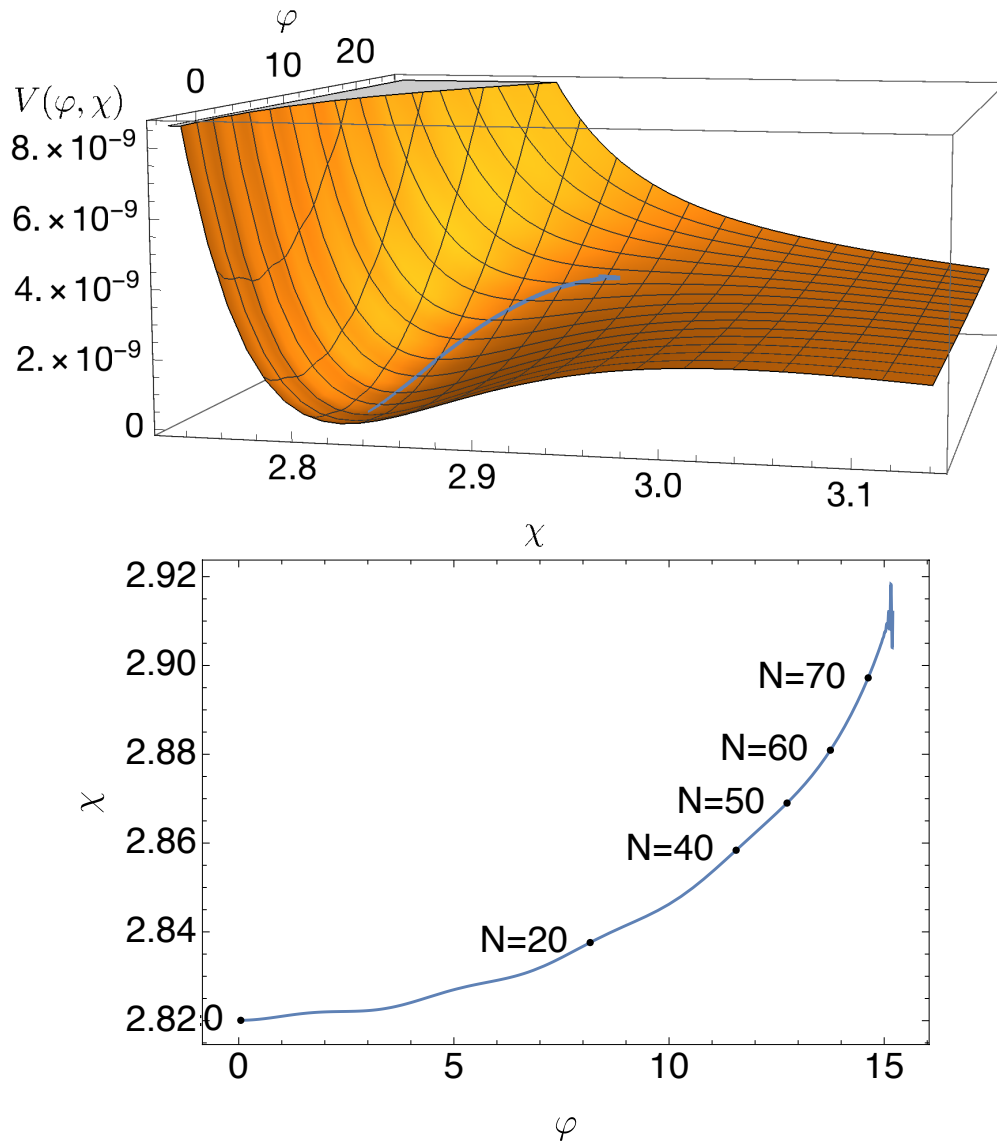


Figure 4: Potential and trajectory in field space for small Γ and large δ .

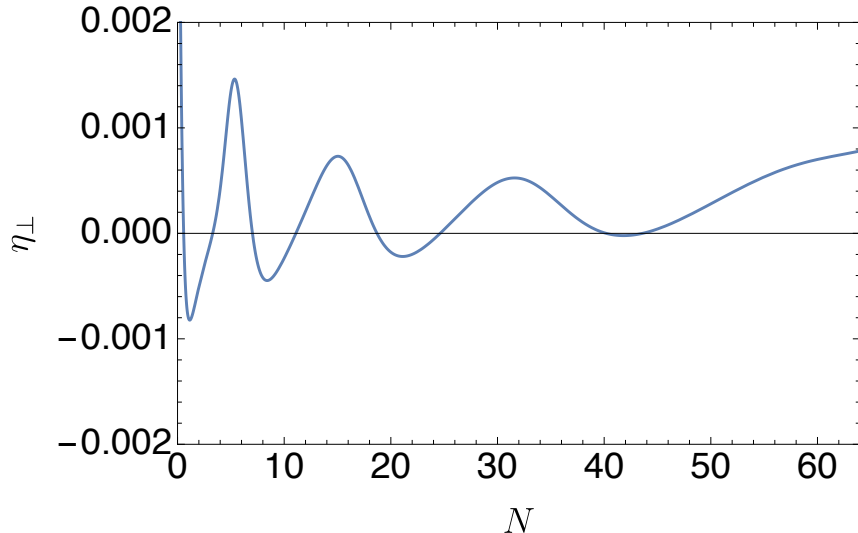


Figure 5: η_{\perp} for the small Γ and large δ case.

In Fig. 6 we can see the typical shape of the power spectra for a given scale, in this case the one that exits the horizon at 57 e -folds. Since η_{\perp} is so small the system is decoupled and, as expected, the adiabatic limit is reached as soon as the scale exits the horizon. In this limit, the curvature perturbation is constant, and the isocurvature perturbation completely negligible. The best way to obtain the constant towards which the curvature perturbation approaches is to evolve the system until the end of Inflation and evaluate the power spectra then. In our model the system is already deep in the adiabatic regime 20 e -foldings after horizon exit. We can see that, at this time, the isocurvature perturbation is many orders of magnitude smaller than the curvature perturbation. Unfortunately, this makes it very hard to perform computations after that. The numerical precision required to perform computations is such that the necessary computer time is too large. Nevertheless, we can clearly see that the system is barely evolving by that time, so we can safely evaluate the power spectra 20 e -foldings after horizon exit. As a further check one can solve the equations in the decoupling limit $\eta_{\perp} \rightarrow 0$, which is always a good approximation in this thesis. In this limit it is easy to evolve the system until the end of Inflation, and this has helped verifying our results.

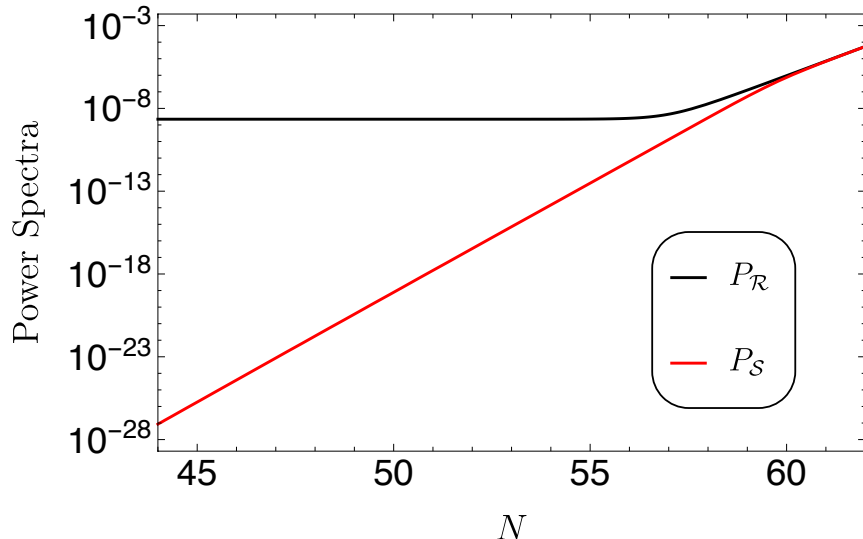


Figure 6: Power spectra for the small Γ and large δ case for the scale that leaves the horizon at $N = 57$. The adiabatic limit is reached as soon as the scale exits the horizon. A few e -foldings after horizon exit the isocurvature perturbation is already 20 orders of magnitude smaller than the curvature perturbation and due to limited computational time we cannot evolve the system beyond this point. We have verified that the results can be extrapolated to the end of Inflation by solving the equations in the decoupling limit, which is a very good approximation in all of the cases we study.

After solving the Mukhanov-Sasaki equations for a large number of scales we obtain the power spectra as a function of time (or N) and the scale k . For the reasons explained above, we need to evaluate the power spectra and the rest of observables once the adiabatic limit is reached. Thus, the cosmological observables are functions only of the scale k . Instead of having the scale in the x -axis, the observables are usually plotted in terms of the number of e -foldings at which the scale exits the horizon. In Fig. 7, Fig. 8 and Fig. 9 we have plotted the spectral tilt, its running and the tensor-to-scalar ratio. We can see that the tilt and the running are inside the observational bounds for the scales of interest. The tensor-to-scalar ratio is a little bit too large to match the observations. This problem is frequent in large-field inflationary models. Among these models, the one we are studying gives a very low r . If tensor modes were soon detected in the CMB observations or through an stochastic background of gravitational waves in the near future, more realistic models inspired in this toy model could still be viable.

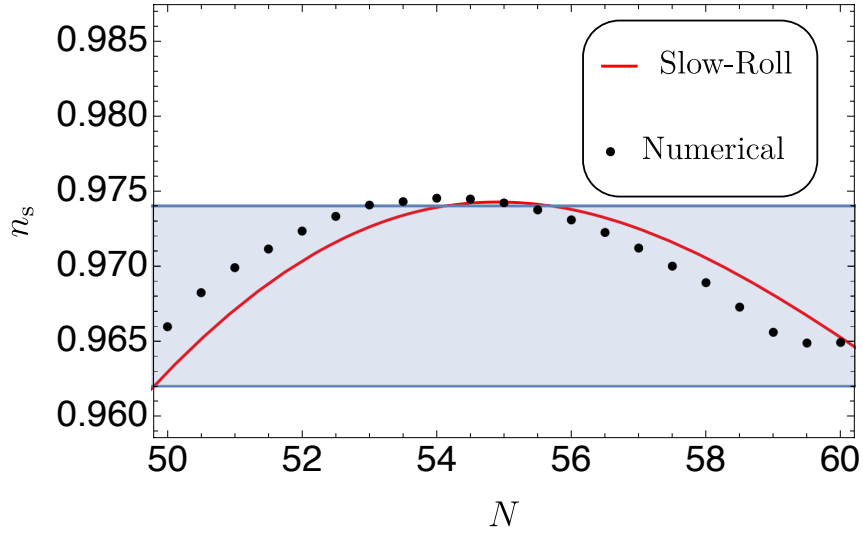


Figure 7: Spectral index at the scales of cosmological interest for the small Γ and large δ case. The oscillations in n_s have a low frequency and a large amplitude.

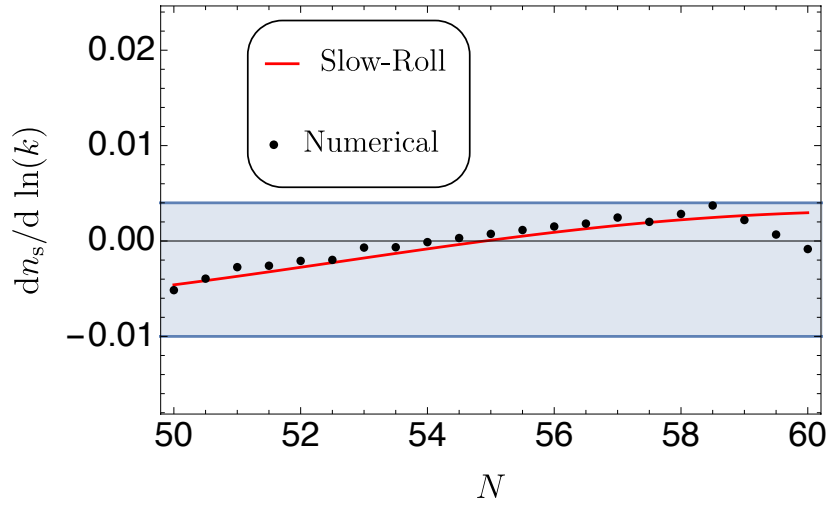


Figure 8: Running of the spectral index at the scales of cosmological interest for the small Γ and large δ case.

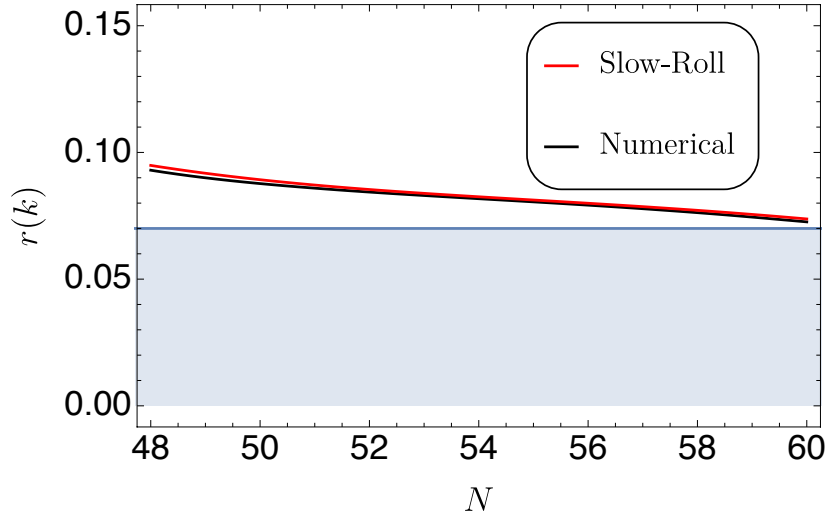


Figure 9: Tensor-to-scalar ratio at the scales of cosmological interest for the small Γ and large δ case.

W_0	W_0/μ	δ	Γ	φ_0	χ_0
0.026	2000	0.001	10	17.8	2.82

Table 2: Set of parameters for large Γ and small δ .

6.2.2 Large Γ and small δ

Let us move on to the example with a larger frequency Γ in Table 2. We have chosen δ as small as required by the observations. Even though the oscillations are faster, they cannot be observed in the potential without changing the scale of the plot in Fig. 10, because its amplitude δ has decreased a lot. The fast oscillations can be seen in η_{\perp} in Fig. 11. This is because we have changed the scale of the plot. Indeed, if we compare it to Fig. 5, we realize that η_{\perp} has decreased by a factor of 100. It is even smaller, so, again, we cannot expect to see multi-field effects. We can also see that the oscillations in the spectral tilt, in Fig. 12, and its running, in Fig. 13, have gotten faster. The numerical results agree quite well with the slow-roll predictions, as expected. In Fig. 14 we see that the tensor-to-scalar ratio is again a bit larger than the present observational bounds.

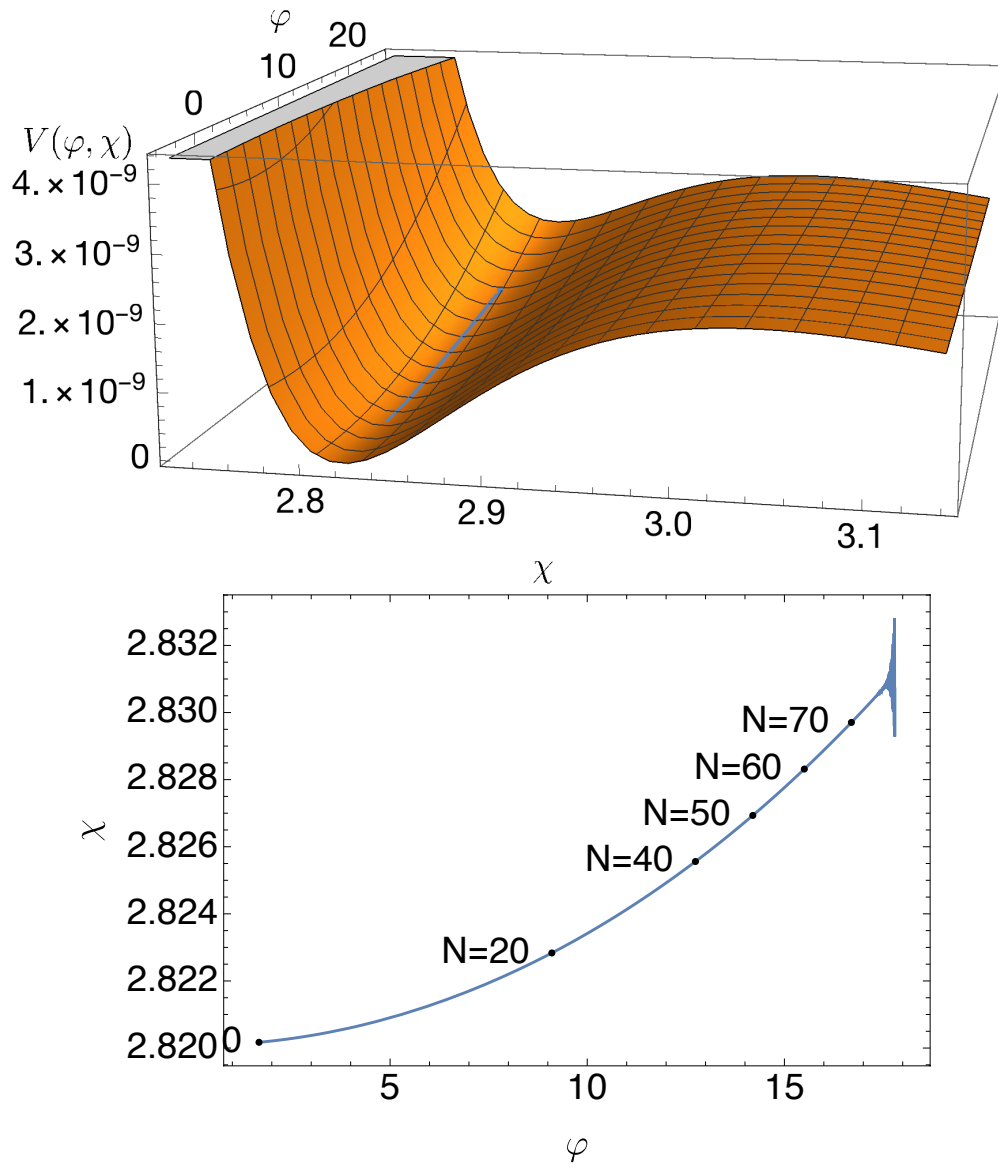


Figure 10: Potential and trajectory in field space for the case of large Γ and small δ .

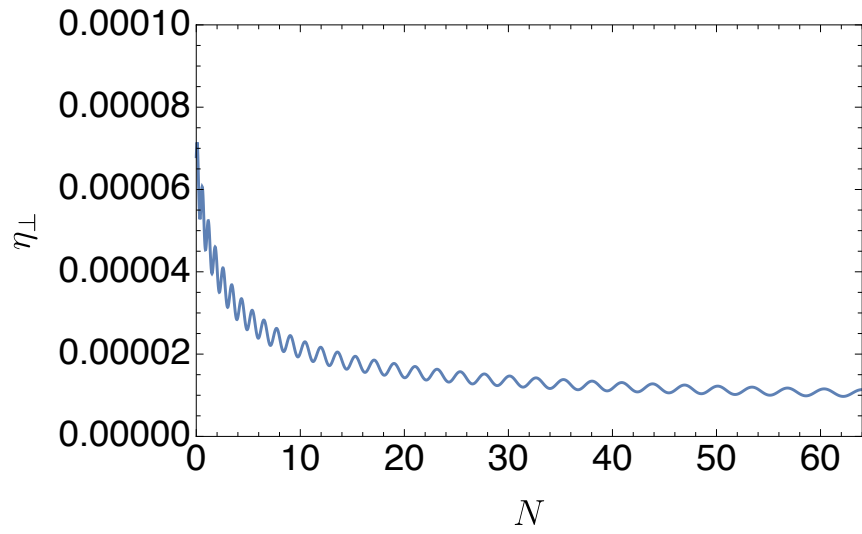


Figure 11: η_{\perp} for the large Γ and small δ case.

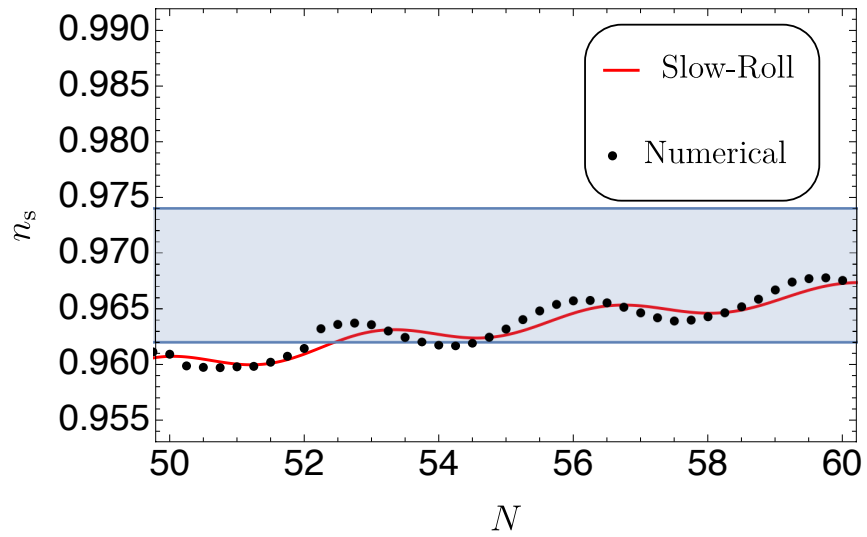


Figure 12: Spectral index at the scales of cosmological interest for the large Γ and small δ case. The oscillations in n_s have a large frequency but a small amplitude.

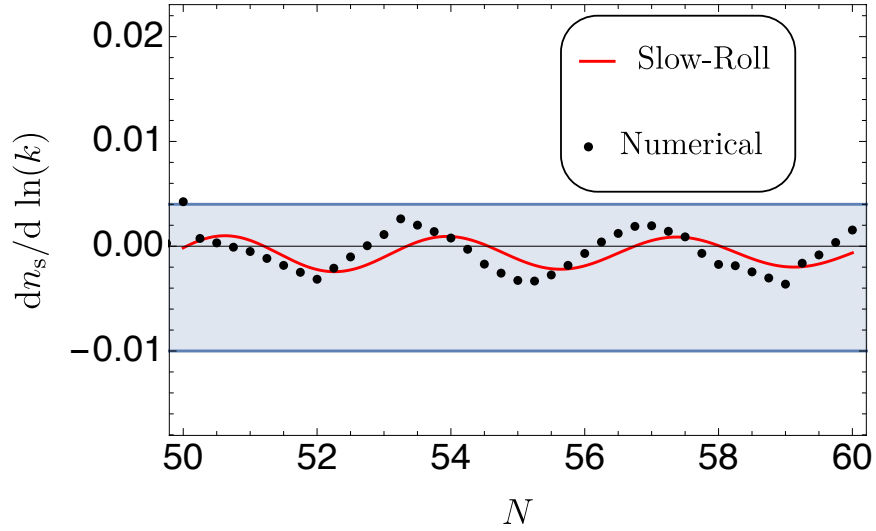


Figure 13: Running of the spectral index at the scales of cosmological interest for the large Γ and small δ case.

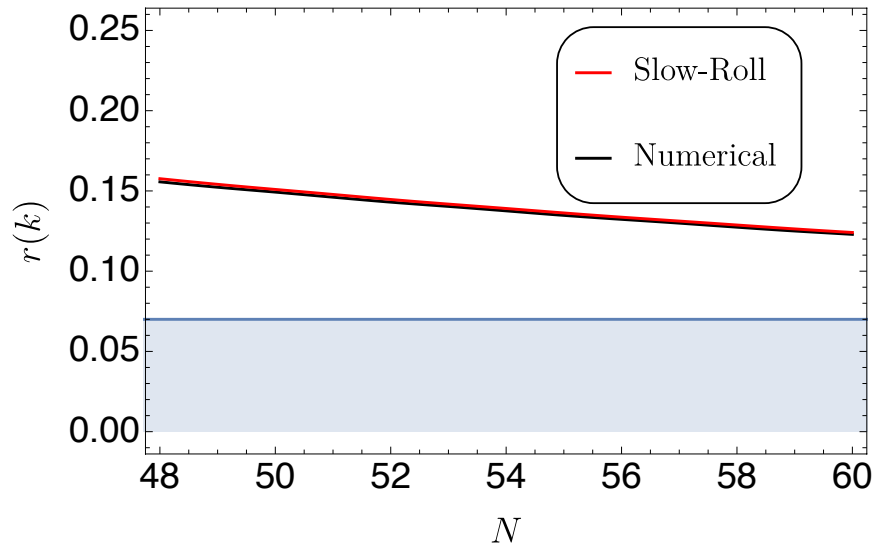


Figure 14: Tensor-to-scalar ratio at the scales of cosmological interest for the large Γ and small δ case.

W_0	W_0/μ	δ	Γ	φ_0	χ_0
0.006	290	0.48	16.35	14.4	2.9

Table 3: Set of parameters for large Γ and large δ .

6.2.3 Large Γ and large δ

Finally, we study an example where both the frequency Γ and the amplitude δ (remember that δ should be smaller than 1) of the corrections are comparably large. The fast oscillations are clearly visible in the potential in Fig. 15. Their effect on the trajectory in field space can also be seen in this figure. As a result, large oscillations appear in η_{\perp} in Fig. 16. Nevertheless, if we compare η_{\perp} with the rest of parameters in Eq. (63), we realize that it is not dominant, so we do not expect to see multi-field effects. We have found that if one increases both δ and Γ at the same time, the fields can get stuck in a local minimum. The system would enter in an eternal false-vacuum inflationary period, which would never give way to Reheating nor the SMC periods. We have also found that, to obtain a large coupling between curvature and isocurvature, one needs both large δ and large Γ . Unfortunately, this predicament prevents us from obtaining multi-field effects, as those obtained in the square potential of section 3.

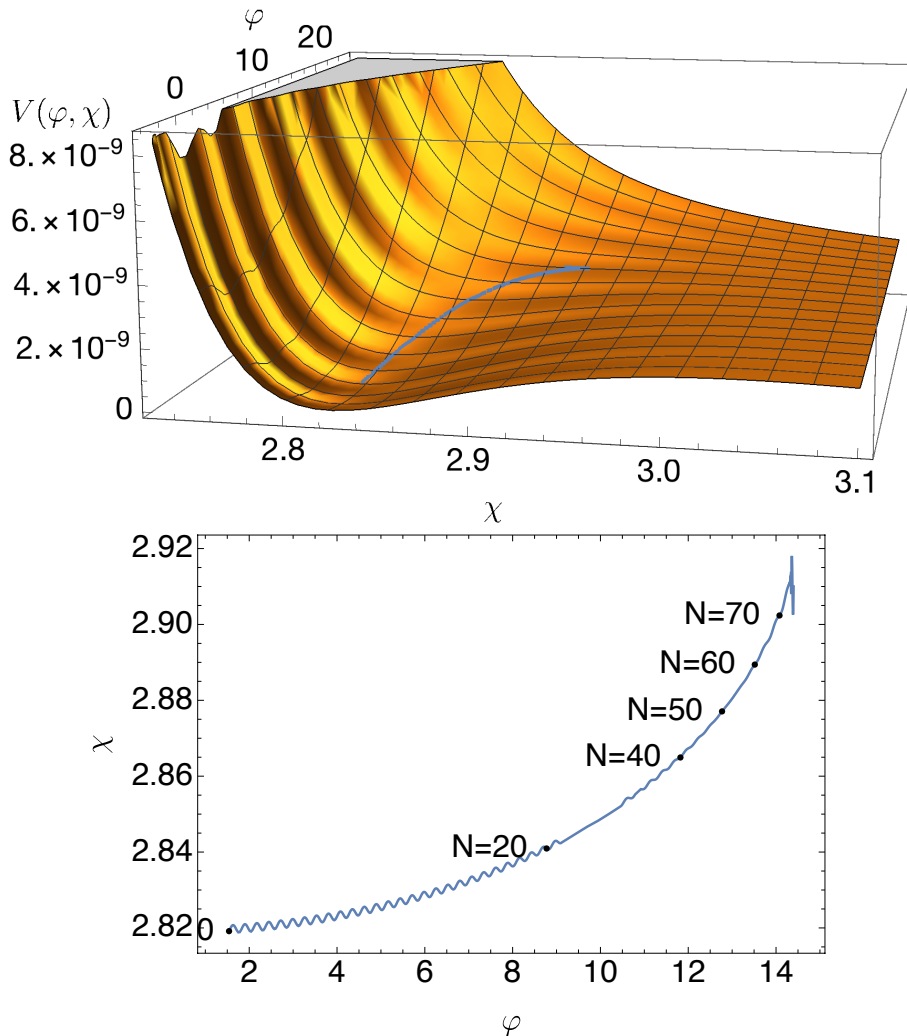


Figure 15: Potential and trajectory in field space for the case of large Γ and large δ .

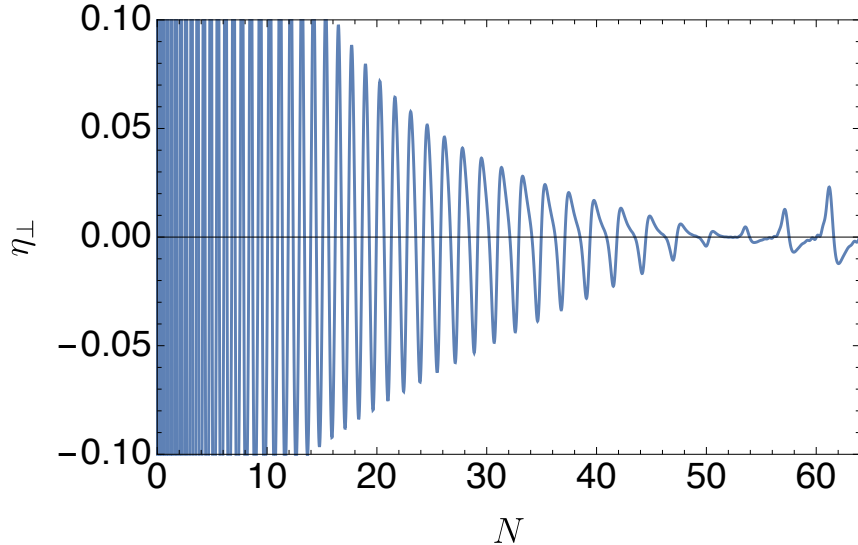


Figure 16: η_{\perp} for the large Γ and large δ case. It is higher than in the other two cases presented above.

Since we are in the decoupling limit, $P_{\mathcal{R}}$ is expected to be frozen far outside the horizon, and this is what we observe in Fig. 17, where we plot the power spectra of curvature and isocurvature perturbations for the scales that leave the horizon at 57 and at 57.25 e -folds. Comparing Fig. 17 and Fig. 6 we notice that in this new example we need to wait a few e -folds before the adiabatic limit is reached. This is a sign that new physics is starting to become relevant. In fact, in Fig. 18, Fig. 19 and Fig. 20, where we have plotted the numerical and the slow-roll predictions for the cosmological observables, we note that there is a strong disagreement between them. In this case we are therefore forced to use the full MS equation to make predictions, since the slow-roll approximation is not valid. Unfortunately, our prediction always crosses the experimental bounds in tiny patches between 50 – 60 e -foldings. Thus, it would require a lot of fine-tuning of our initial conditions to get the precise number of e -foldings to meet the observations. Furthermore, these windows do not coincide for all the observables, they are actually mutually exclusive. Consequently, this parameter regime is ruled out by observations.

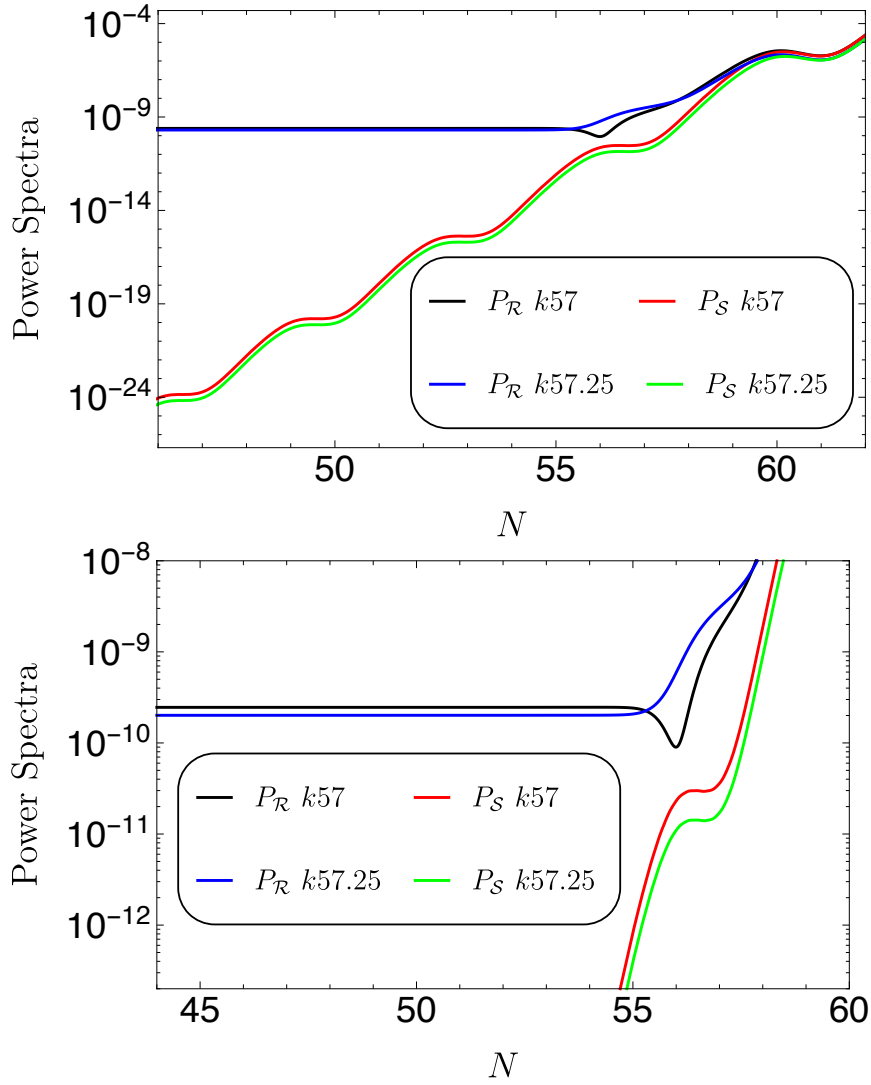


Figure 17: Power spectra for the large Γ and large δ case for the scales that leave the horizon at $N = 57$ and $N = 57.25$. Bunch-Davies initial conditions are imposed at 62 e -folds, when the scales are well inside the horizon and the curvature and isocurvature perturbations coincide. They starting evolving while being sub-horizon, in a wavy manner, expected from the oscillatory nature of the potential. We need to wait around 3 e -folds until the adiabatic limit is reached.

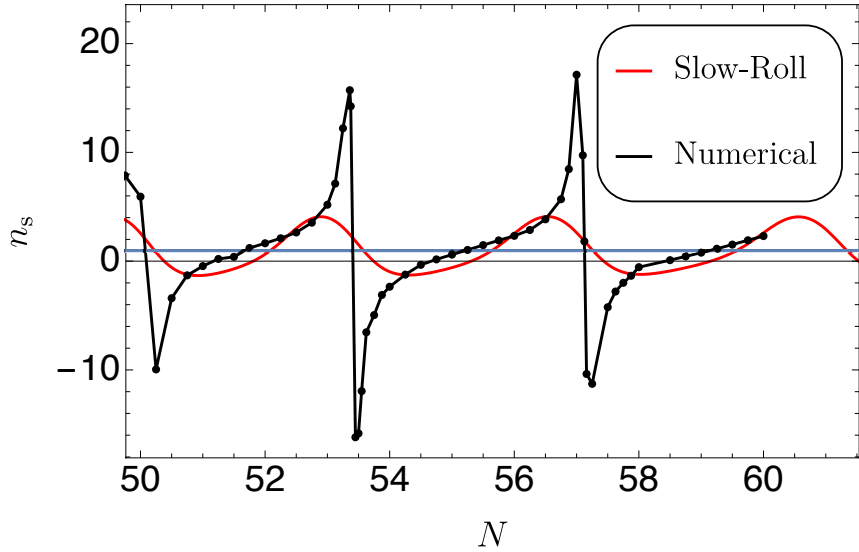


Figure 18: Spectral index at the scales of cosmological interest for the large Γ and large δ case. The experimental bounds are seen as a blue line, due to the exaggerated scale of the plot. The patches where our prediction matches the observations are so small that a great deal of fine-tuning would be needed to get the number of e -foldings right. The choice of parameters is, of course, completely unphysical, but the plot illustrates well the fact that the slow-roll equations cannot be used to predict observables. The oscillations in n_s have a large frequency and a large amplitude.

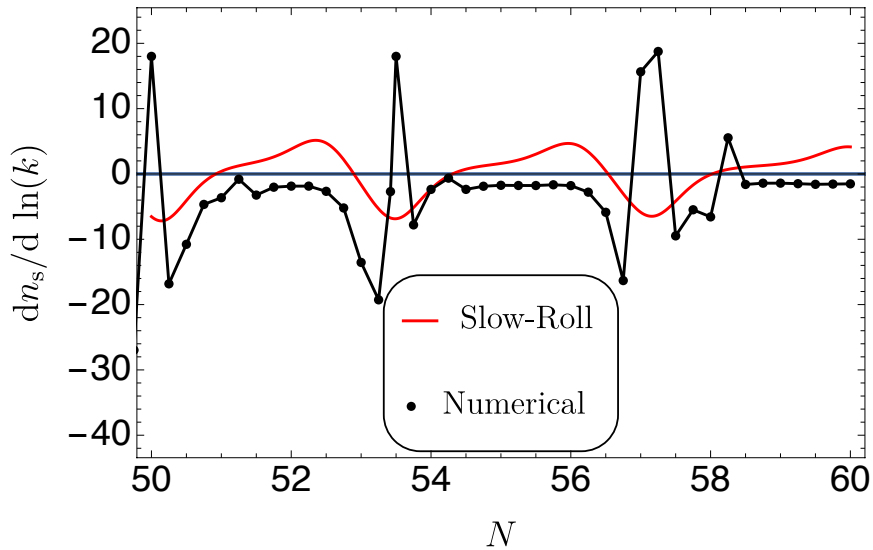


Figure 19: Running of the spectral index at the scales of cosmological interest for the large Γ and large δ case. The experimental bounds are seen as a blue line, due to the exaggerated scale of the plot as in Fig. 18. The patches where our prediction matches the observations are so small that a great deal of fine-tuning would be needed to get the number of e -foldings right. Again, we observe a difference between the slow-roll and the numerical prediction.

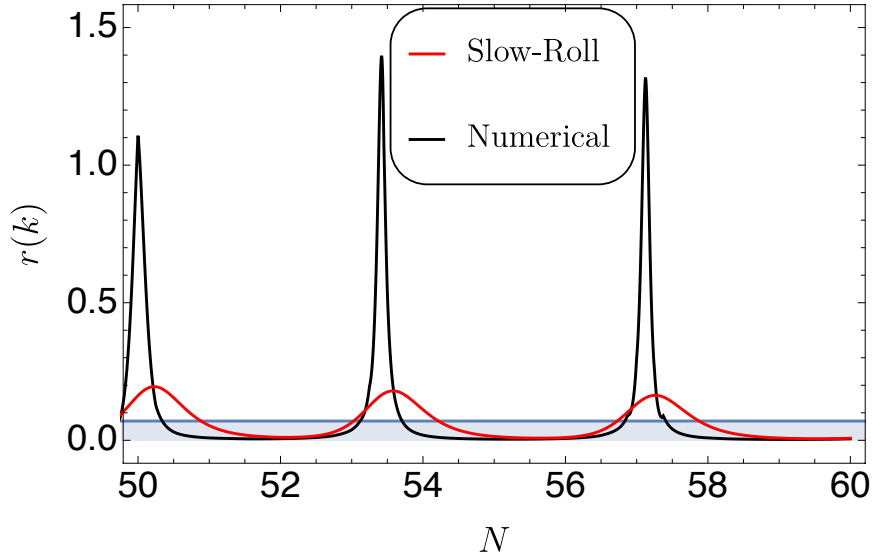


Figure 20: Tensor-to-scalar ratio at the scales of cosmological interest for the small Γ and large δ case. Again, we observe a mismatch between the slow-roll and the numerical prediction.

6.2.4 Comparing the examples

We have found that the model is able to match the observations only if the amplitude of the oscillations is small. If we increase Γ , then we need to decrease δ in such a way that the strength of the oscillations remains constant. Otherwise, the predictions fall outside the experimental window. In the first two examples we were able to produce realistic models. As can be seen by comparing their parameters in Tables 1 and 2, in order to still be able to account for the observations after increasing Γ by a factor of 10 one needs to decrease δ by a factor of 100. The importance of this result can be appreciated if we remember Eq. (106) for the superpotential: if we include high-frequency corrections, then the experimental data forces them to be highly suppressed.

In all of our examples we are in the decoupling limit. However, only in the last example we have a disagreement between the numerical and the slow-roll prediction. In Fig. 21 we can see the slow-roll parameter η_{\parallel} for the three examples. Only the last example breaks the slow-roll condition $\eta_{\parallel} \ll 1$. This means that in this last case we cannot use the slow-roll formulas to make predictions.

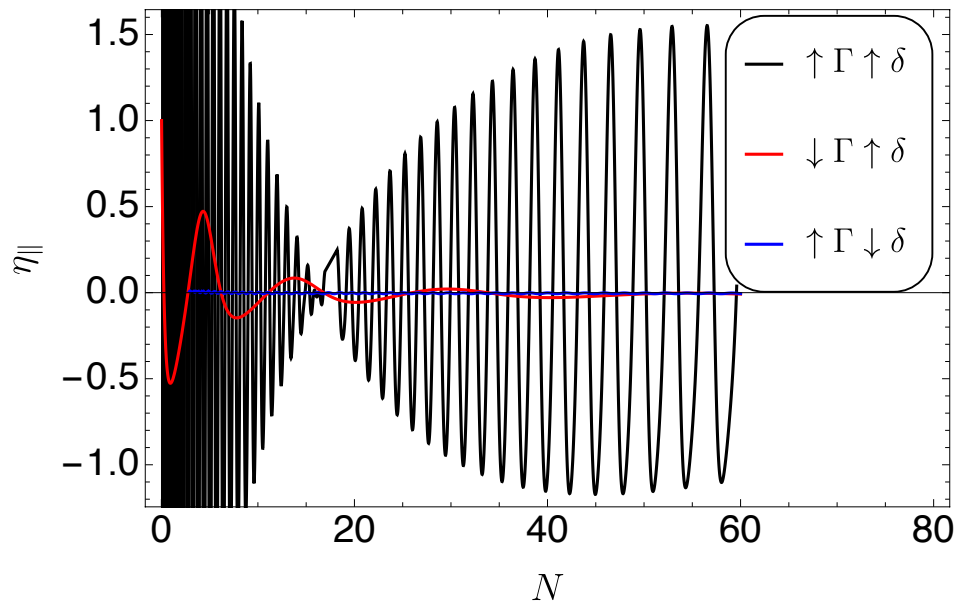


Figure 21: Comparison of $\eta_{||}$ for the three examples. The slow-roll approximation is valid in the first two cases, but not in the last one.

7 Conclusions

We have studied the cosmological observables predicted by the two-field toy model of [8]. Our efforts were focused on studying the effects that the one-loop correction to the non-perturbative term in the superpotential has on the cosmological observables. In particular, we have studied the case where this term is given by simple sines and cosines.

- First, we were able to obtain realistic models with high-frequency but small-amplitude oscillations and also with small-frequency but large-amplitude ones. In both cases the fields are weakly coupled, which means that there are no multi-field effects associated with the bends of the trajectory. Moreover, they are in the slow-roll regime, which means that we can use the slow-roll, single-field equations and ignore all the other detailed predictions which could have potentially appeared through the multi-field MS equations. In these examples we have observed oscillations in the cosmological observables, induced by the corrections we are interested in.
- Then, we went on exploring the parameter space, searching for signatures of multi-field dynamics. Unfortunately, when we tried to make the corrections larger, so as to increase η_{\perp} , the fields started to get stuck on local minima. Thus, our perturbations remain always weakly coupled. We were able to check that, as the corrections started to increase, the slow-roll approximation started to fail. In our last example, it was necessary to solve the MS equation to compute the cosmological observables. Approximately, at the same time the slow-roll approximation started to fail, the predictions started to fall outside the experimental windows.

Even though our model was not able to predict evidence for multi-field dynamics while correctly predicting the cosmological observables, the findings of this project are still very interesting and could pave the way for more sophisticated analyses. For example, we have been able to keep our approximations under control, and have been able to understand when the full multi-field equations are needed.

We have been able to appreciate the shortcomings of our model by fully understanding the role of each parameter in the potential and its effects on the cosmological observables. Namely, we have been able to understand the interplay between the amplitude and the frequency of these oscillations: we can only match the experimental observations by keeping one of them small. In addition, we have verified that the parameter W_0 can be adjusted to give the scalar perturbations its proper amplitude.

As a summary, to increase the coupling between curvature and isocurvature we need our trajectory to bend, thus giving a large value of η_{\perp} . To do this, we would need faster ($\uparrow \Gamma$) and

larger ($\uparrow \Gamma, \uparrow \delta$) oscillations, which would create wells in the potential deep enough to trap the system in a local minima. Although this prevents us from observing multi-field effects, we can still observe oscillations large enough to break slow-roll. However, in this case, our model is excluded by observations, since it predicts fast and large oscillations in the tilt of the curvature power spectra. This means that if we include high-frequency corrections in the superpotential, then the experimental data forces them to be highly suppressed.

We believe that the physical insight gained in this project can be very useful in constructing other similar models of Inflation. Let us summarize what assumptions of the thesis could be changed, what other ideas may be introduced through further studies and to what extent our findings can be applied to them.

- First of all, we have assumed that the one-loop corrections to the non-perturbative term in W appear through a hyperbolic sine function, but in many scenarios it can be a more complicated periodic function, such as θ -functions. In other scenarios, also explored in ref. [8], it can be non-periodic, and include exponentials and polynomial functions. For example, in this reference it is shown that, if the coefficient is a polynomial, there can be a single very sharp turn in the trajectory. In this case we expect η_{\perp} to peak there and help us identify multi-field effects. If we are able to study several simple cases we may be able to put them together in a realistic model full of string-theory, multi-field signatures.
- Secondly, it would also be interesting to search for setups without the tree-level contribution $\mu\Phi^2$ to W but some other power law, or even a more complicated function. Then, we can ask ourselves how this affects the one-loop corrections. Regarding the perturbative terms, it would be rewarding to gain a better understanding of the one-loop correction. To do this we cannot start already with our toy model for the Kähler potential and the superpotential, we need to go back and choose a specific scenario. This could be achieved by choosing a simple manifold with fluxes, a certain D-brane configuration and then solving explicitly the one-loop string diagrams.
- Finally, we have been assuming that the full moduli stabilization has been carried out. It would be comforting to be able to do it for an explicit flux background and make sure that nothing relevant changes.

Unveiling the physics behind Inflation is one of the most exciting open problems in Theoretical Physics. At the moment, all we have are bounds on the tensor-to-scalar ratio, r . There are many ongoing experiments like Advanced LIGO, Advanced VIRGO, KAGRA, LIGO India or, in the next few decades, experiments like LISA, that will provide additional information and decrease the experimental windows. Moreover, future experiments like PIXIE, COrE or BICEP3

could determine the tensor perturbations of Inflation by studying the polarization of the CMB. According to the simplest inflationary models, the detection of an inflation-related stochastic background of Gravitational Waves will probably have to wait until the next-to-next-generation of space-based observatories, like Big Bang Observatory (BBO) and maybe Deci-hertz Interferometer Gravitational wave Observatory (DECIGO) [18]. A detection of this background would provide extremely useful information about the early Universe. It would help to differentiate inflationary models, ruling out entire model families. It would also probe some aspects of the quantum nature of fields and gravity.

As our understanding of String Theory improves, it may be possible to explore higher-energy scenarios of Inflation. There is much to be learned by exploring these new regimes, where many new signatures of the theory may eventually appear. String Theory could be the UV theory behind Inflation and we need to keep learning as much as we can about it so as to be ready when the experiments finally come through.

References

- [1] W. Buchmuller, E. Dudas, L. Heurtier, A. Westphal, C. Wieck, and M. Winkler, JHEP 04, 058 (2015), 1501.05812. .
- [2] S. Davis and M. Postma, JCAP 0803, 015 (2008), 0801.4696. .
- [3] R. Kallosh, A. Linde, K. Olive, and T. Rube, Phys.Rev. D84, 083519 (2011), 1106.6025. .
- [4] W. Buchmuller, C. Wieck, and M. Winkler, Phys.Lett. B736, 237 (2014), 1404.2275. .
- [5] W. Buchmuller, E. Dudas, L. Heurtier, and C. Wieck, JHEP 09, 053 (2014), 1407.0253. .
- [6] E. Dudas and C. Wieck, JHEP 10, 062 (2015), 1506.01253. .
- [7] S. Bielleman, L. Ibanez, F. Pedro, I. Valenzuela, and C. Wieck, Higgs-otic Inflation and Moduli Stabilization, 10.1007/JHEP02 (2017) arXiv:1611.07084 .
- [8] F. Ruehle and C. Wieck, One-loop Pfaffians and large-field inflation in String Theory, Physics Letters B (Volume 769, Pages 289-298, 10 June 2017).
- [9] S. Weinberg, *Cosmology*, Oxford University Press, 2008.
- [10] J. Garcia Bellido, Astrophysics and Cosmology, in *Invited Lectures at 1999 European School of High Energy Physics, Casta-Papiernicka, Slovak Republic*. arXiv:hep-ph/0004188, 2000.
- [11] S. Dodelson, *Modern Cosmology*, Academic Press, 2003.
- [12] C. Bennett et al., [WMAP Collaboration] Nine-Year Wilkinson Microwave Anisotropy Probe (WMAP) Observations: Final Maps and Results, *Astrophys. J. Suppl.* 208, 20 [arXiv:1212.5225]. (2013).
- [13] R. Adam et al., [Planck Collaboration] Planck 2015 results. Cosmological parameters, *Astron. Astrophys.* 594, A1 [arXiv:1502.01582] (2016).
- [14] F. Albareti et al., [SDSS Collaboration] The Thirteenth Data Release of the Sloan Digital Sky Survey: First Spectroscopic Data from the SDSS-IV Survey Mapping Nearby Galaxies at Apache Point Observatory, Submitted to *ApJS* (2016).
- [15] C. S. Kochanek et al., Results from the CASTLES survey of gravitational lenses, in *AIP Conference Proceedings* 470, 163 (1999).
- [16] S. Perlmutter et al., Cosmology from Type Ia Supernovae, Jan '98 AAS Meeting, also cited as BAAS,29,1351. astro-ph/9812133 (1997).

- [17] www.elisascience.org/.
- [18] N. Bartolo et al., Science with the space-based interferometer LISA. IV: probing inflation with gravitational waves, *Journal of Cosmology and Astroparticle Physics (JCAP)*, Volume 2016, December 2016 .
- [19] www.bicepkeck.org/.
- [20] V. Mukhanov, *Physical Foundations of Cosmology*, Cambridge University Press, 2005.
- [21] D. H. Lyth and A. R. Liddle, *The primordial density Perturbation*, Cambridge University Press, 2009.
- [22] D. Baumann, *TASI Lectures on Inflation*, arXiv:0907.5424, 2009.
- [23] D. Baumann and L. McAllister, *Inflation and String Theory*, Cambridge University Press, 2016.
- [24] V. Mukhanov, H. A. Feldman, and R. H. Brandenberger, Theory of cosmological perturbations, *Physics Reports*, Volume 215, Issue 5-6, p. 203-333. (1992).
- [25] C. Patrignani et al., *The Review of Particle Physics*, Particle Data Group, *Chin. Phys. C*, 40, 100001 (2016) and 2017 update.
- [26] A. Achúcarro et al., Features of heavy physics in the CMB power spectrum, *JCAP* 1101 (2011) 030 arXiv:1010.3693 .
- [27] S. Bielleman, L. Ibanez, F. Pedro, and I. Valenzuela, Multifield Dynamics in Higgs-otic Inflation, *JHEP* 1601 (2016) 128 arXiv:1505.00221 .
- [28] I. Huston and A. Christopherson, Calculating Non-adiabatic Pressure Perturbations during Multi-field Inflation, *Phys. Rev. D* 85, 063507 (2012) .
- [29] L. E. Ibanez and A. M. Uranga, *String Theory and Particle Physics*, Cambridge University Press, 2012.
- [30] J. Polchinski, *String Theory Vol. 1: An Introduction to the boson string, Vol. 2: Superstring theory and beyond*, Cambridge University Press, 1998.
- [31] M. Green, J. Schwarz, and E. Witten, *Superstring Theory. Vol. 1: Introduction and Vol.2 Loop Amplitudes, Anomalies and Phenomenology*, Cambridge University Press, 1987.
- [32] J. Wess and J. Bagger, *Supersymmetry and Supergravity*, Princ, 1992.

- [33] S. Giddings, S. Kachru, and J. Polchinski, Hierarchies from Fluxes in String Compactifications, *Phys. Rev. D*, 106006 (2002), hep-th/0105097 .
- [34] S. Kachru, R. Kallosh, A. Linde, and S. Trivedi, de Sitter Vacua in String Theory, *Phys. Rev. D* 68, 046005 (2003), hep-th/0301240 .
- [35] C. Burgess, M. Majumdar, D. Nolte, F. Quevedo, G. Rajesh, and R. Zhang, *JHEP* 0107 (2001) 047 [hep-th/0105204] .
- [36] C. Burgess, Lectures on cosmic Inflation and its Potential Stringy Realizations, in *arXiv:0708.2865*, 2007.